Hydrol. Earth Syst. Sci. Discuss., 12, 11959–12037, 2015
www.hydrol-earth-syst-sci-discuss.net/12/11959/2015/
doi:10.5194/hessd-12-11959-2015

Hydrology and Earth System Sciences
Open Access
Discussions

A comprehensive one-dimensional numerical model for solute transport in rivers

M. Barati Moghaddam, M. Mazaheri, and J. M. V. Samani

Department of Water Structures, Tarbiat Modares University, Tehran, Iran

Received: 4 October 2015 – Accepted: 18 October 2015 – Published: 17 November 2015

Correspondence to: M. Mazaheri (m.mazaheri@modares.ac.ir)

Published by Copernicus Publications on behalf of the European Geosciences Union.

Abstract

Interactions between physical and chemical mechanisms involved in pollutant transport in rivers occur with varying degrees, depending on flow discharge and physical conditions. One of the issues that greatly affect the transport, especially in small mountain streams, is transient storage zones. The main effects include temporary retention of pollutants and reduce its concentration at the downstream and indirect impact on sorption process in the streambed. This paper proposes a one-dimensional model to simulate the pollutant transport in rivers with irregular cross-sections under unsteady flow with transient storage zones. The proposed model verified with analytical solution and comparison with 2-D model. The model application shown by two hypothetical examples and four set of real data that covers different processes governing on transport, cross-section types and flow regimes. Comparing results of the model with two common contaminant transport models show good accuracy and numerical stability of the model than other ones.

1 Introduction

First efforts to understanding the solute transport issue, leading to longitudinal dispersion theory, is often referred to as classical advection-dispersion equation (ADE) (Taylor, 1954). This equation is a parabolic partial differential equation and obtained from combination of continuity equation and Fick's first law. One-dimensional ADE equation is as follows:

$$\frac{\partial(AC)}{\partial t} + \frac{\partial(CQ)}{\partial x} = \frac{\partial}{\partial x}\left(AD\frac{\partial C}{\partial x}\right) - A\lambda C + AS \quad (1)$$

where, A = flow area, C = solute concentration, Q = volumetric flow rate, D = dispersion coefficient, λ = first-order decay coefficient, S = source, t = time and x = distance.

When this equation is used to simulate transport in prismatic channels and rivers with relatively regular and uniform cross-sections, good results have been achieved. but

HESSD
12, 11959–12037, 2015

field studies, particularly in mountain pool-and-riffle streams, indicates that observed concentration-time curves have a lower peak concentration and longer tails than ADE equation predictions (Godfrey and Frederick, 1970; Nordin and Sabol, 1974; Nordin and Troutman, 1980; Day, 1975). Thus a group of researchers based on field study results, stated that to accomplish more accurate simulation of solute transport in natural river and streams, ADE equation must be modified and some terms added to it for consideration the impact of stagnant areas-that so-called storage zones (Bencala et al., 1990; Bencala and Walters, 1983; Jackman et al., 1984; Runkel, 1998; Czernuszenko and Rowinski, 1997; Singh, 2003). Transient storage zones, mainly includes eddies, stream poolside areas, stream gravel bed, streambed sediments, porous media of channel bed and banks and stagnant areas behind flow obstructions such as big boulders, stream side vegetation, woody debris and so on.

In general, these areas affect pollutant transport in two ways: on one hand, by temporary retention and gradual release of solute, causing an asymmetric shape in the observed concentration-time profiles, that could not be explained by classical advection-dispersion theory and on the other hand by providing the opportunity for reactive pollutants to repeated contact with streambed sediments, indirectly affect solute sorption process and makes it more intensive, especially in low flow conditions (Bencala, 1983, 1984; Bencala et al., 1990; Bencala and Walters, 1983).

So far, several approaches have been proposed to simulate the solute transport in rivers with storage areas, that one of the most commonly used is transient storage model (TSM). Transient storage mathematical model has been developed to show solute movement from main channel to stagnant zones and vice versa. The simplest form of TSM is One-dimensional advection-dispersion equation with an additional term to transient storage (Bencala and Walters, 1983). Since the introduction of TS model, transient storage processes have been studied in variety of small mountain streams to big rivers and shown that simulation results of tracer study data with considering transient storage impact have good agreement with real data. Also, interactions between main channel and storage zone, especially in mountain streams have great ef-

HESSD
12, 11959–12037, 2015

fect on solute transport behavior (D'Angelo et al., 1993; DeAngelis et al., 1995; Morrice et al., 1997; Czernuszenko et al., 1998; Chapra and Runkel, 1999; Chapra and Wilcock, 2000; Laenen and Bencala, 2001; Fernald et al., 2001; Keefe et al., 2004; Ensign and Doyle, 2005; Van Mazijk and Veling, 2005; Gooseff et al., 2007; Jin et al., 2009).

The objective of this study is to present a comprehensive model that merges numerical schemes with higher order accuracy for solving one-dimensional advection-dispersion equation with transient storage and kinetic sorption in rivers with irregular cross-sections under unsteady flow condition that obviate shortcomings of common models of pollutant transport. The presented model for providing a comprehensive modeling framework couples three sub-models of calculating geometric properties of irregular cross sections, solving unsteady flow equations and solving transport equations with transient storage and kinetic sorption.

For demonstrating of applicability and accuracy of model, results for two hypothetical examples and four set of real data, compared with the results of two current solute transport models, the MIKE11 model (that uses classical ADE equation for solute transport simulation) and OTIS model that today is the only existed model for solute transport with transient storage (Runkel, 1998).The presented model and two other models properties in comparison with each other are given in Table 1.

As obvious from Table 1, the presented model have advantages of both other models at the same time, whereas does not have their disadvantages. For example, OTIS in simulation of transport in irregular cross-sections under non-uniform or unsteady flow has to rely on an external stream routing program and geometric properties and flow data must be interred the model from another routing program in the form of text file. However in the presented and MIKE11 models, geometric properties and unsteady flow data, are directly evaluated from river topography, bed roughness, flow initial and boundary condition data. Also the presented model in this study has the ability to simulate solute transport problem in both with and without transient storage conditions under steady and unsteady flow regimes and in rivers with irregular cross section –

HESSD
12, 11959–12037, 2015

without limitation in section number – that from this aspect is unique among solute transport models presented so far.

Another important point is the numerical scheme that used in model structure. Table 2 specifies comparison of numerical schemes that used in structure of three subjected models. The key and basic difference of the presented model with two other models is in spatial discretization of transport equations. The presented model uses control volume approach and QUICK scheme in spatial discretization of advection-dispersion equation with transient storage and kinetic sorption, whereas the two other models implement that by central spatial differencing. As many of researchers claims, central spatial differencing, is unable in simulation of pure advection problem and does not show good performance (Zhang and Aral, 2004; Szymkiewicz, 2010), while QUICK scheme is better than the central scheme one (Neumann et al., 2011).

It should be mentioned that, in recent years QUICK scheme has been widely used in spatial differencing for ADE equation, due to its high-order accuracy (from third order), very small numerical dispersion and having higher stability rang, in particular in the case of pure advection dominant transport than other numerical methods (Neumann et al., 2011; Lin and Medina Jr., 2003). Hence usage of QUICK scheme in numerical discretization of transport equation leads to significant superiority of the presented model to two other models, especially in advection dominant problems.

2 Material and methods

2.1 Governing differential equations

Transient storage model is a simplified mathematical framework of complex physical processes of transport in a natural river or stream. There are several equations for solute transport with transient storage, which among them, the transient storage model presented by Bencala and Walters (1983), used in this study, because of its ability to consider the unsteady flow regime and irregular cross-sections. By writing conserva-

HESSD
12, 11959–12037, 2015

tion of mass equations for solute in main channel and storage zone, a coupled set of differential equations for main channel and storage zone is derived:

$$\frac{\partial C}{\partial t} = \frac{-Q}{A}\frac{\partial C}{\partial x} + \frac{1}{A}\frac{\partial}{\partial x}\left(AD\frac{\partial C}{\partial x}\right) + \frac{q_{\mathrm{LIN}}}{A}(C_{\mathrm{L}} - C) + \alpha(C_{\mathrm{S}} - C) \quad (2)$$

$$\frac{\mathrm{d}C_{\mathrm{S}}}{\mathrm{d}t} = \alpha\frac{A}{A_{\mathrm{S}}}(C - C_{\mathrm{S}}) \quad (3)$$

where A and A_{S} are the main channel and storage zone cross-sectional area; C, C_{L} and C_{S} are the main channel, lateral inflow and storage zone solute concentration, respectively; q_{LIN} is the lateral inflow rate; α is the storage zone exchange coefficient. For reactive (or non-conservative) solute, with considering two types of chemical reactions; kinetic sorption and first-order decay, Eqs. (2) and (3) are re-written as:

$$\frac{\partial C}{\partial t} = L(C) + \rho\hat{\lambda}\,(C_{\mathrm{Sed}} - K_{\mathrm{d}}C) - \lambda C \quad (4)$$

$$\frac{\mathrm{d}C_{\mathrm{S}}}{\mathrm{d}t} = S(C_{\mathrm{S}}) + \hat{\lambda}_{\mathrm{S}}\left(\hat{C}_{\mathrm{S}} - C_{\mathrm{S}}\right) - \lambda_{\mathrm{S}}C_{\mathrm{S}} \quad (5)$$

where $\hat{C}_{\mathrm{S}}$ is the background storage zone solute concentration; C_{Sed} is the sorbate concentration on the streambed sediment; K_{d} is the distribution coefficient; λ and λ_{S} are the main channel and storage zone first-order decay coefficient; $\hat{\lambda}$ and $\hat{\lambda}_{\mathrm{S}}$ are the main channel and storage zone sorption rate coefficient, respectively; ρ is the mass of accessible sediment/volume water; $L(C)$ and $S(C_{\mathrm{S}})$ are the right-hand side of Eqs. (2) and (3) respectively. There is another variable concentration in Eq. (4), C_{Sed}, which a mass balance equation is required:

$$\frac{\mathrm{d}C_{\mathrm{Sed}}}{\mathrm{d}t} = \hat{\lambda}(K_{\mathrm{d}}C - C_{\mathrm{Sed}}). \quad (6)$$

HESSD
12, 11959–12037, 2015

2.2 Numerical solution of 1-D advection-dispersion equation with transient storage and kinetic sorption

Numerical solution of Eqs. (4)–(6), in this study are based on control volume method and centered time-QUICK space (CTQS) scheme. The spatial derivatives are discrete by QUICK scheme and average of n and $n+1$ time levels. QUICK scheme is based on quadratic upstream interpolation for discretization of advection-dispersion equation (Leonard, 1979). In this scheme, face values are obtained from quadratic function passing through two upstream nodes and a downstream node. In a uniform grid, the value of desired quantity at the cell face is given by following equations:

$$\phi_{\text{face}} = \frac{6}{8}\phi_{i-1} + \frac{3}{8}\phi_i - \frac{1}{8}\phi_{i-2} \tag{7}$$

$$\text{if } u_{\text{w}} > 0: \quad \phi_{\text{w}} = \frac{6}{8}\phi_{\text{W}} + \frac{3}{8}\phi_{\text{P}} - \frac{1}{8}\phi_{\text{WW}} \tag{8}$$

$$\text{if } u_{\text{e}} > 0: \quad \phi_{\text{e}} = \frac{6}{8}\phi_{\text{P}} + \frac{3}{8}\phi_{\text{E}} - \frac{1}{8}\phi_{\text{W}} \tag{9}$$

where P denotes to the unknown nodes with neighbor nodes to the west and east are identified by W and E respectively. The west side control volume face is referred to by w and the east side face of control volume by e. The dispersion terms are evaluated using the gradient of the approximating parabola. Since the slope of chord between two points on a parabola is equal to the slope of the tangent to the parabola at its midpoint, on a uniform grid with equal control volumes, dispersion terms are the same as expressions of central differencing for dispersion, therefore:

$$\left(\frac{\partial\phi}{\partial x}\right)_{\text{w}} = \frac{\phi_{\text{P}} - \phi_{\text{W}}}{\Delta x} \tag{10}$$

$$\left(\frac{\partial\phi}{\partial x}\right)_{\text{e}} = \frac{\phi_{\text{E}} - \phi_{\text{P}}}{\Delta x}. \tag{11}$$

HESSD
12, 11959–12037, 2015

The discretized form of Eqs. (4)–(6) are written as Eqs. (12)–(14):

$$\frac{C_{\mathrm{P}}^{n+1}-C_{\mathrm{P}}^{n}}{\Delta t}=\frac{1}{2}\left[\left(\frac{-Q_{\mathrm{P}}}{A_{\mathrm{P}}\Delta x}(C_{\mathrm{e}}-C_{\mathrm{w}})\right)^{n+1}+\left(\frac{-Q_{\mathrm{P}}}{A_{\mathrm{P}}\Delta x}(C_{\mathrm{e}}-C_{\mathrm{w}})\right)^{n}\right] \tag{12}$$
$$+\frac{1}{2}\left\{\frac{1}{A_{\mathrm{P}}^{n+1}\Delta x}\left[\left(AD\frac{\partial C}{\partial x}\right)_{\mathrm{e}}-\left(AD\frac{\partial C}{\partial x}\right)_{\mathrm{w}}\right]^{n+1}\right.$$
$$\left.+\frac{1}{A_{\mathrm{P}}^{n}\Delta x}\left[\left(AD\frac{\partial C}{\partial x}\right)_{\mathrm{e}}-\left(AD\frac{\partial C}{\partial x}\right)_{\mathrm{w}}\right]^{n}\right\}$$
$$+\frac{1}{2}\left[\frac{q_{\mathrm{LIN}}^{n+1}}{A_{\mathrm{P}}^{n+1}}(C_{\mathrm{L}}-C_{\mathrm{P}})^{n+1}+\frac{q_{\mathrm{LIN}}^{n}}{A_{\mathrm{P}}^{n}}(C_{\mathrm{L}}-C_{\mathrm{P}})^{n}\right]$$
$$+\frac{\alpha}{2}\left[(C_{\mathrm{S}}-C_{\mathrm{P}})^{n+1}+(C_{\mathrm{S}}-C_{\mathrm{P}})^{n}\right]$$
$$+\frac{\rho\hat{\lambda}}{2}\left[(C_{\mathrm{Sed}}-K_{\mathrm{d}}C_{\mathrm{P}})^{n+1}+(C_{\mathrm{Sed}}-K_{\mathrm{d}}C_{\mathrm{P}})^{n}\right]-\frac{\lambda}{2}\left(C_{\mathrm{P}}^{n+1}+C_{\mathrm{P}}^{n}\right)$$

$$\frac{C_{\mathrm{S}}^{n+1}-C_{\mathrm{S}}^{n}}{\Delta t}=\frac{1}{2}\left[\left(\alpha\frac{A_{\mathrm{P}}}{A_{\mathrm{S}}}(C_{\mathrm{P}}-C_{\mathrm{S}})+\hat{\lambda}_{\mathrm{S}}\left(\hat{C}_{\mathrm{S}}-C_{\mathrm{S}}\right)-\lambda_{\mathrm{S}}C_{\mathrm{S}}\right)^{n+1}\right. \tag{13}$$
$$\left.+\left(\alpha\frac{A_{\mathrm{P}}}{A_{\mathrm{S}}}(C_{\mathrm{P}}-C_{\mathrm{S}})+\hat{\lambda}_{\mathrm{S}}\left(\hat{C}_{\mathrm{S}}-C_{\mathrm{S}}\right)-\lambda_{\mathrm{S}}C_{\mathrm{S}}\right)^{n}\right]$$

$$\frac{C_{\mathrm{Sed}}^{n+1}-C_{\mathrm{Sed}}^{n}}{\Delta t}=\frac{1}{2}\left[\left(\hat{\lambda}\left(K_{\mathrm{d}}C_{\mathrm{P}}-C_{\mathrm{Sed}}\right)\right)^{n+1}+\left(\hat{\lambda}\left(K_{\mathrm{d}}C_{\mathrm{P}}-C_{\mathrm{Sed}}\right)\right)^{n}\right]. \tag{14}$$

By substitution the values on control face from Eqs.(8)–(11) and doing some algebraic operations, Eq. (12) can be written as:

$$a_{\mathrm{WW}}C_{\mathrm{WW}}^{n+1}+a_{\mathrm{W}}C_{\mathrm{W}}^{n+1}+a_{\mathrm{P}}C_{\mathrm{P}}^{n+1}+a_{\mathrm{E}}C_{\mathrm{E}}^{n+1}=R_{\mathrm{P}}. \tag{15}$$

HESSD
12, 11959–12037, 2015

For solving the resultant system of linear equations, all of the quantities that appear on the right hand side of Eq. (15) should be known, hence the quantities of storage zone concentration and the sorbate concentration on the streambed sediment at the advanced time level (C_{Sed}^{n+1}, C_{S}^{n+1}), should be evaluated by using Eqs. (13) and (14) as:

$$C_{\mathrm{S}}^{n+1} = \frac{\gamma_{\mathrm{P}}^{n+1} C_{\mathrm{P}}^{n+1} + \gamma_{\mathrm{P}}^{n} C_{\mathrm{P}}^{n} + \left(2 - \Delta t \lambda_{\mathrm{S}} - \gamma_{\mathrm{P}}^{n}\right) C_{\mathrm{S}}^{n}}{2 + \gamma_{\mathrm{P}}^{n+1} + \Delta t \lambda_{\mathrm{S}}} \tag{16}$$

$$\gamma = \frac{\alpha \Delta t A}{A_{\mathrm{S}}}$$

$$C_{\mathrm{Sed}}^{n+1} = \frac{\left(2 - \Delta t \hat{\lambda}\right) C_{\mathrm{Sed}}^{n} + \Delta t \hat{\lambda} K_{\mathrm{d}} \left(C_{\mathrm{P}}^{n} + C_{\mathrm{P}}^{n+1}\right)}{2 + \Delta t \hat{\lambda}}. \tag{17}$$

If the number of control volumes in solution domain be N, writing Eq. (15) for each four successive control volumes, from third to $N-1$th control volume, results a set of equations with $N-3$ equation and N unknowns. For solving this set of equations three more equations is needed, which yield from upstream and downstream boundary conditions. In QUICK scheme the concentration quantities at control faces calculated by using of concentration values in three adjacent nodes, two nodes at upstream and one node at downstream. Nodes 1, 2 and N all for the reason of locating the proximity of domain boundaries and implementation of boundary conditions, need to be treated separately. Equation (18) shows the matrix form of the resultant system of equations. By solving this system of equations, main channel concentrations in $n+1$ time level are obtained. Having main channel concentration values, storage zone and streambed sediment concentrations could be evaluated from Eqs. (16) and (17) for all control volumes.

HESSD
12, 11959–12037, 2015

$$\begin{bmatrix} a_P & a_E & & & & & & \\ a_W & a_P & a_E & & & & & \\ a_{WW} & a_W & a_P & a_E & & & & \\ & a_{WW} & a_W & a_P & a_E & & & \\ & & & \vdots & \vdots & \vdots & \vdots & \\ & & & \vdots & \vdots & \vdots & \vdots & \\ & & & \vdots & \vdots & \vdots & \vdots & \\ & & & & a_{WW} & a_W & a_P & a_E \\ & & & & & a_{WW} & a_W & a_P \end{bmatrix} \begin{bmatrix} C_1 \\ C_2 \\ C_3 \\ C_4 \\ \vdots \\ \vdots \\ \vdots \\ C_{N-1} \\ C_N \end{bmatrix} = \begin{bmatrix} R_1 \\ R_2 \\ R_3 \\ R_4 \\ \vdots \\ \vdots \\ \vdots \\ R_{N-1} \\ R_N \end{bmatrix} \quad (18)$$

2.3 Damköhler index

For assuring that transient storage happens in designed hypothetical examples, Damköhler number was used. This criterion is a dimensionless number that reflects the exchange rate between main channel and storage zones (Jin et al., 2009; Harvey and Wagner, 2000; Wagner and Harvey, 1997; Scott et al., 2003). For a stream or channel with length L, DaI is written as:

$$\mathrm{DaI} = \frac{\alpha(1 + A/A_S)L}{u}. \quad (19)$$

When DaI is much greater than unity, for example 100, the exchange between main channel and storage zone is too fast that could be assumed that these two segments are in balance. When DaI is much lower than unity, for example 0.001, the exchange rate between main channel and storage zone is very low and negligible. In the other words, in such a stream where DaI is very low, practically there is no significant exchange between main channel and storage zone and transient storage does not affect downstream solute transport. It showed that for a reasonable estimation of transient storage model parameters, the DaI value must be between 0.1 to 10 (Fernald et al., 2001; Wagner and Harvey, 1997; Ramaswami et al., 2005).

HESSD
12, 11959–12037, 2015

3 Model verification

The presented model is verified by analytical solution of advection-dispersion equation with transient storage for two type of upstream boundary condition (continuous and Heaviside) and also by comparing the model results with 2-D model ones. The characteristics of hypothetical examples for model verification have been shown in Table 3.

3.1 Verification by analytical solution

In this section, model verification, carried out by using an analytical solution that presented by Kazezyılmaz-Alhan (2008). She developed analytical solutions for the transient storage model introduced by Bencala and Walters (1983), for both continuous and finite source boundary conditions, assuming that flow velocity, channel cross-sectional area and longitudinal dispersion coefficient do not change with respect to time, with no lateral inflows, and first order decay in main channel and storage zone. Table 4 shows characteristics of designed hypothetical examples. DaI dimensionless number is obtained as 0.8, thus selected parameters are considered correct.

3.1.1 Upstream boundary condition: continuous

In this case, a solute concentration of 5 mg m^{-3} is injected continuously for 10 h. Computational time and space steps assumed 30 s and 1 m, respectively. Figure 1 shows the numerical model results compare to analytical solution at 50, 75 and 100 m form upstream. Error indexes for continuous contaminant boundary condition are given in Table 5. According to Fig. 1 and error indexes of Table 5, it is clear that the trends of numerical and analytical solutions of transient storage equations are similar and also the presented model shows acceptable precision in this example.

As previously mentioned the presented model has the ability of solute transport simulation in both with and without storage cases. Hence, in order to show model capabilities and assess the model results accuracy in without transient storage case, the

HESSD
12, 11959–12037, 2015

model is implemented with $\alpha = 0$ for this example and results compared to analytical solutions of classic advection-dispersion equation. For instance, results are shown in Fig. 2, in the form of comparative concentration-time curves in two cases of with and without storage at 100 m from upstream. Table 6 presents error indexes for continuous boundary condition, in both with and without transient storage simulation. It can be seen from Fig. 2 that the model results, in both cases, are very close to analytical solutions. Error indexes of Table 6, also confirm it. This figure also illustrate that in the case of with transient storage, concentration-time curves have lower peak than the without storage ones ($\alpha = 0$), that matches the previously mentioned transient storage concept.

3.1.2 Upstream boundary condition: Heaviside function

This time, a solute concentration of 5 mg m^{-3} is injected to the stream for a limited time of 100 min. Total time of simulation was 10 h, also time and space steps assumed 30 s and 1 m, respectively. Comparison of model results with analytical solutions illustrated in Fig. 3. Table 7 shows error indexes for this simulation. Figure 3 and Table 7 confirm the reliability of model results.

After assuring the correctness of simulation results in the case of Heaviside upstream boundary condition with transient storage, the model is implemented for this example with $\alpha = 0$ and obtained results compared with analytical solution of classic advection-dispersion equation. Results are given in Fig. 4, as comparative concentration–time curve at 100 m from upstream. Error indexes for simulation with and without storage are presented in Table 8. According to Fig. 4, it is obvious that the model results in both cases (with and without storage) have reasonable fitness with analytical solution and both results follow a similar trend. This figure also clearly shows difference between solute concentration-time curves in two cases. When storage affects downstream solute transport, these curves show lower peak and longer tail than without storage transport ones.

HESSD
12, 11959–12037, 2015

3.2 Verification by 2-D model

A 2-D model due to consideration of velocity variations in two dimensions of river reach, gives more accurate predictions of transport and behavior of solute in reality. For verification of the presented model using 2-D model, a hypothetical example was designed, a 1200 m length river with irregular cross-sections. Figure 5 illustrates bathymetry properties of hypothetical river. As clear in the figure, in the distance of 300 to 600 m the river has obvious wide variation. In fact for creation of hypothetical storage zone, river in this section have been widened as unilateral.

The total time of simulation is equal to 14 h and the flow condition in river is unsteady and non-uniform. Also in this example the flow assumed to be subcritical, thus for model implementation boundary conditions at each upstream and downstream points are needed. The boundary conditions of flow sub-model are volumetric flow rate and water level variations with respect to time at upstream boundary ($x = 0$ m) and downstream boundary ($x = 1200$ m), respectively. For creation of flow initial condition, flow sub-model was implemented for 14 h with constant flow discharge and depth, that equals to their values at $t = 0$ (cold-start). Implementation of transport model also needs initial condition and two boundary conditions. Upstream and downstream boundary conditions are step loading and zero-gradient concentration, respectively.

The solute concentration in main channel and storage zone, at the beginning of simulation, assumed to be zero. In calculations of both flow and transport models, space step (Δx) and time step (Δt) are 100 m and 1 min, respectively. Other characteristics of hypothetical example such as Manning's roughness coefficient, longitudinal dispersion coefficient, storage zone area and exchange coefficient are showed in Table 9. Dal number is obtained to be 0.4 for this example, thus chosen parameters are correct and acceptable. Model results for simulations with and without transient storage in compare with 2-D model results, at different distances from upstream, illustrated in Fig. 6. This figure shows that with appropriate A_S and α, concentration-time curves with transient storage is so close to the 2-D model results curve. These results indicates the neces-

HESSD
12, 11959–12037, 2015

sity of considering transient storage terms in advection-dispersion equation for more accurate simulation of solute transport especially in natural river and streams, again.

In the following, for showing the higher accuracy of numerical method that used in the presented model, the results of three models, CTQS, CTCS and BTCS in compare with 2-D model ones, are presented. Figure 7a and b shows that the CTQS model results are closer to 2-D model results compared to two other model ones. That means that with considering appropriate parameters for storage zone area and exchange coefficient, the presented model is capable of estimating observed concentration-time curves in natural river and streams with sufficient and reasonable precision. For detailed comparison, error indexes are given in Table 10. These error indexes show that among all three mentioned methods, CTQS method has less error percentage and more accuracy than the two other ones. Also the trend of CTQS method results is much more like the 2-D model ones than the other.

4 Application

In this section, the application of presented model and comparison of the results with the ones of OTIS and MIKE11 models are presented by using of hypothetical examples and several sets of real data. General characteristics of these examples are given in Table 11. As shown in table, the chosen examples include the wide variety of solute transport simulation applications at different flow regimes in various cross-section types (regular and irregular) and physical and chemical transport processes.

4.1 Example 1: pure advection

In order to demonstrate the advantages of numerical method used in the proposed model, for advection dominant problems, a hypothetical example designed and three numerical schemes CTQS, CTCS and BTCS were implemented for this purpose. The results are shown and compared in the form of concentration-time curves. Steady flow

HESSD
12, 11959–12037, 2015

with $10\,m^3\,s^{-1}$ volumetric rate and regular cross-sections with $10\,m^2$ area were assumed. Total time of simulation was 5 h, space and time steps were 100 m and 10 s, respectively. Due to that advection is the only affective process in transport, the effect of dispersion and transient storage were ignored (dispersion coefficient assumed to be very small and near to zero).

According to Figs. 8 to 10 it is clear that, for pure advection simulation, the CTQS scheme has less oscillation than the two other ones. In particular, as illustrated in Fig. 9, the results of CTCS scheme that also used in OTIS numerical model structure have very high oscillations, while the CTQS scheme results show very little oscillations and higher numerical stability. Therefore it can be said that the presented model for advection dominant simulation has better performance than the two other models. It is interesting to note, that mountain rivers where transient storage mechanism also more observed in such rivers, due to relatively high slope, have higher flow velocities than plain rivers, and as a result advection is the dominant process in solute transport. Thus these results somehow confirm the superiority of presented model for simulation of solute transport with transient storage compared to the common models.

4.2 Example 2: transport with first-order decay

This example illustrates the application of presented model in solute transport simulation undergoing first-order decay without transient storage and kinetic sorption in the form of a hypothetical problem. A decaying substance enters the stream with steady and uniform flow during a 2 h period. The solute concentration at the upstream boundary is 100 concentration units. Other characteristics of the problem are given in Table 12. Also in order to assess model capabilities in the case of high flow velocity and advection dominant, as the Peclet number is the measure for advection relative power, this problem performed in 3 cases with different Peclet numbers. The properties of three model implementation cases are given in Table 13.

HESSD
12, 11959–12037, 2015

Figures 11 to 13 show simulation results of three numerical models in compare to analytical solution. Error indexes are given in Tables 14 and 15. It is obvious from Fig. 11a to c that in the first case (Peclet number less than 2), all methods simulated concentration time profile with same accuracy. Also, Fig. 11d to f show that MIKE11 model have a little flaws in simulation of concentration-space profile than two other models, as Table 15 indexes confirm it. In the second case, by increasing computational space step, all methods show falling in peak concentration, that its amount for MIKE11 model is more and for the presented model is less than the others (see Fig. 12a to c). Figure 12d to f and Table 15 indexes demonstrate that the results of models that used from central differencing scheme in spatial discretization of transport equations, show more discrepancy with analytical solution.

In the third case, flow velocity increased about four times. As illustrated in Fig. 13c, by increasing Peclet number, the OTIS model results show more oscillations in proximity of the edges. This model results also show very intense oscillations in concentration-space profile in the form of negative concentrations (Fig. 13e), while observed oscillations in the presented model is very small compared to OTIS model (Fig. 13d). However QUICK scheme oscillations in advection dominant cases, are less likely to corrupt the solution. Figure 13c and f presents that MIKE 11model results in compare to the proposed model have greater difference with analytical solutions.

The reason of difference between model results in the three cases, actually related to how advection and dispersion affect the solute transport. The dispersion process affects the distribution of solute in all directions, whereas advection spreads influence only in the flow direction. This fundamental difference manifests itself in the form of limitation in computational grid size. Numerical schemes with central spatial differencing produce spurious oscillations for certain problems such as high flow velocities and advection dominant transport. One way to overcome these oscillations is the use of finer grids, with the choice of space step based on the dimensionless Peclet number. Spatial discretization in a Peclet number smaller than 2 can eliminate numerical oscillations and Peclet number less than 10 can reduce such oscillation, greatly. However

HESSD
12, 11959–12037, 2015

the more computational cost due to extensively fine grid may become impractical in some applications, particularly in natural river and streams. While quadratic upstream interpolation schemes such as QUICK scheme that used in the proposed model, is designed in the way that overcomes this oscillatory behavior. These schemes simulate the problem with reasonable accuracy even with greater space steps in compare to central differencing ones (Versteeg and Malalasekera, 2007).

4.3 Example 3: conservative solute transport with transient storage

This example shows the presented model application to field data, by using the conservative tracer (chloride) injection experiment results, which was conducted in Uvas Creek, a small mountain stream in California. Injection of concentrated NaCl solution started in 08:00 LT of 26 September 1972 and continued for 3 h. During the experiment, flow discharge in Uvas Creek was near to seasonal base-flow, approximately to 12.5 $L s^{-1}$, non-uniform and steady flow. Chloride background concentration recorded 3.7 $mg L^{-1}$. Five sampling sites established in 38, 105, 281, 433 and 619 m downstream of injection point, respectively (Avanzino et al., 1984). Table 16 shows simulation parameters for Uvas Creek experiment such as reach length, dispersion coefficient, discharge, main channel and storage zone cross sectional area and exchange coefficient for each reach (Bencala and Walters, 1983). For assessing of efficiency and accuracy of three discussed models in simulation of the impact of physical processes (advection, dispersion and transient storage) on solute transport in a mountain stream, they are implemented for this set of real date.

Figure 14a to c illustrates simulated chloride concentration in main channel by using three mentioned models. It can be seen from figure and Table 17 indexes, that the presented model simulated the experiment results more accurate than the two other ones. Comparison of Fig. 14a and b show that the CTQS and OTIS models have good precision in modeling the peak concentration and the CTQS model has better performance in simulation of rising tail of concentration-time curve, particularly in 281 m station. Figure 14c shows MIKE11 model results. Due to using classical AD equation

HESSD
12, 11959–12037, 2015

and ignoring the effect of transient storage process, its results show significant discrepancy with observed data, particularly in peak concentrations. However at 38 m station, where transient storage does not affect solute transport ($\alpha = 0$), the results of three models have little difference with observed data (Table 17).

Figure 15 demonstrates the model results for Uvas Creek experiment for simulation with and without transient storage at 281 and 433 m stations. This figure shows that in simulation with transient storage, the results have more fitness with real data in general shape of concentration–time curve, peak concentration and peak arrival time. Figure 16 shows the simulated chloride concentrations in storage zone. As it is obvious from the figure, the concentration–time curves in storage zone have longer tails in compare to main channel ones. That means some portions of solute mass remain in storage zones, after passing the solute pulse and when completely passage of pulse from stream occurs, gradually return to the main channel takes place. Because of these mechanisms the concentration–time curves in main channel have lower peak and longer tails than the predicted ones from classical advection-dispersion equation.

Figure 17 indicates the transient storage concept that mentioned later, in the form of observed data. This figure shows that gradually from the beginning of simulation, the main channel solute concentrations decrease and add to storage zone concentrations. In other words, at first storage zone acts as a sink and after passage of solute pulse becomes a source of solute. If longer simulation time assumed, for example several days or even weeks, balancing in the main channel and storage zone concentrations and return to background concentrations, can be observed. This example shows the impact of physical processes on solute transport and the necessity of considering transient storage effect in natural river and streams transport modeling, for obtaining more accurate results. At next example combined effect of physical and chemical processes on solute transport will be discussed.

HESSD
12, 11959–12037, 2015

4.4 Example 4: non-conservative solute transport with transient storage

The objective of this example is demonstration of the presented model capabilities in non-conservative solute transport modeling in natural rivers and showing how physical and chemical processes affecting transport. For this purpose, the characteristics of a field experiment of the three-hour reactive tracer (Strontium) injection into the Uvas Creek were used. The experiment conducted at low-flow condition, so due to high opportunity of solute for frequent contact with relatively immobile streambed materials, solute and streambed interactions and its sorption into bed sediments was more intense than during the high flow conditions. Hence sorption process must be considered in simulation of this experiment (Bencala, 1983).

Simulation parameters are given in Table 18. Interesting point about this table data is the significant difference between the value of sorption rate coefficient in main channel and storage zone due to their completely different features of these two zones. The mass of accessible sediment/volume water (ρ) assumed in first and last reach is 4×10^4 and at other reaches 2×10^4. Other simulation parameters such as reach length, dispersion coefficient, flow discharge, cross-sectional area of main channel and storage zone and exchange coefficients, are the same as Table 16 parameters.

Figure 18a to c shows solute transport simulation results in this stream by Three examined models in compare to observed data. According to Fig. 18 it could be say that the presented model results show better and more reasonable compatibility with observed data in general shape, peak concentration and peak arrival time. Presented error indexes in Table 18 also confirm it. Figure 18c clearly shows that simulation without transient storage and kinetic sorption in MIKE11 model, leads to very different results from real data. These model results, especially at 38 m station which the exchange coefficient with storage zone assumed to be zero, demonstrate the direct effect of sorption on transport in the form of fall in peak concentration.

Figure 19 illustrates CTQS and OTIS model results for sorbate concentrations on the streambed sediments vs. observed data at 105 and 281 m stations. As it is clear

HESSD
12, 11959–12037, 2015

from Fig. 19 and Table 20 indexes, the CTQS model results have better fitness with observed data that could be related to difference in numerical methods that used in models structure. Figure 20 presented Strontium sorbate concentrations at three various time of simulation (beginning, middle and the end of it) at all sampling stations. This figure clearly shows the solute sorption to and desorption from the bed sediments. At 38 and 105 m stations, which do not have storage zones ($\alpha = 0$), variation in concentration levels between the middle of simulation to the end of it, is too high. It means that a lot of amount of sorbate Strontium rapidly return to the stream water in this period of time, however in other station which have storage zones, this process is slower. Particularly at 619 m station that exchange with storage zone is more than others (due to greater exchange coefficient and storage cross -sectional area than other stations), it can be seen that even with to the end of simulation, amount of sorbate concentration increased while desorption does not occurs yet. In other words, presence of storage zones delays Strontium desorption from bed sediments. This happens because of the longer time combination of Strontium transport into the storage zone, it's desorption and returns to main channel, compare to solute pulse passage duration.

4.5 Example 5: solute transport with transient storage in a river with irregular cross-sections

This example shows the model application for a river with irregular cross-sections under unsteady flow condition. Putz and Smith (2000) describe properties of two field injection experiments at a 26 km length reach from Athabasca River near Hinton, Alberta, Canada. At first injection, 20 % Rhodamin WT continuously injected to the river for 5.25 h with constant discharge and at second one, a slug input tracer test was conducted and the samples were collected in four cross-sections downstream of injection point, means 4.725, 11.85, 16.275 and 20.625 km (Putz and Smith, 2000).In this study the data of slug tracer injection experiment have been used. The simulation reach length is 8.3 km, between 4.725 to 13.025 km of river. The geometric parameters be-

HESSD
12, 11959–12037, 2015

tween two cross-sections, where the survey data does not exist, calculated from linear interpolation of two adjacent sections for a known water level.

The fundamental point in selecting this reach, is it must have common geometric features of rivers with storage zones, such as pool-and-riffle consequently and significant and sudden width variations. Total time of simulation is 10 h, space and time step are 25 m and 1 min respectively. Cross sectional area and exchange coefficient for 5.5 to 6.250 km interval, assumed 40 m^2 and 6×10^{-4}, respectively. Transient storage parameters obtained from trial and error and visually determining of simulation results to experimental data. According to estimated parameters, DaI obtained as 3.8, which are in acceptable domain, therefore it could be say that transient storage affects downstream solute transport in simulation reach.

The flow model boundary conditions are constant flow discharge 334 $m^3 s^{-1}$ at upstream and constant water surface elevation of 952.6 m, according to the Environment Canada gauging station. Since samples were collected just in four cross-sections downstream of the injection site, given concentration-time curve at 4.725 km used as the upstream boundary condition of transport model and the concentration-time curve taken at 11.85 km were used to compare the model results with real data. Downstream boundary condition of transport model was zero-gradient concentration.

Figure 21 shows Athabasca experiment simulation results at 11.85 km from upstream by using three models. Error indexes also are given in Table 21. According to Fig. 21a and Table 21, it can be said that concentration-time curve resulted from implementation of proposed and OTIS models, fit very well with observed tracer concentration-time curve, but the concentration-time curve simulated using the MIKE 11 model has great difference with observed data. Higher MRE index indicates a poor performance of classical ADE equation in simulation of solute transport in natural rivers. Thus in order to more accurate simulation of solute transport in natural rivers, it is necessary that the impact of transient storage on solute downstream transport be considered.

HESSD
12, 11959–12037, 2015

4.6 Example 6: solute transport with hyporheic exchange under unsteady flow condition

This example shows application of the proposed model to simulate solute transport in irregular cross-sections stream, under unsteady flow regime. Most of solute transport models, in order to simplify the work process, flow is considered to be steady. While in most natural rivers, unsteady flow conditions is common and ignoring spatial and temporal flow rate variations and consequently a change in the geometry properties of cross-sections, may lead to incorrect results from solute transport simulation. Tracer study that used in this section, conducted in January 1992 at Huey creek located in the of McMurdo valleys, Antarctica. The stream has a complex hydrological system, because the flow rate changes with respect to temperature and radiation variations, either daily or seasonal (Runkel et al., 1998). Because of it, flow rate was variable from 1 to 4 cubic feet per second during the experiment. Since this stream does not have obvious surface storage zones, cross-sectional area of storage zone and the exchange rate with this area, actually represents the rate of hyporheic exchange and interaction of surface and subsurface water. LiCl tracer at the rate of 8.7 $mL\,s^{-1}$ was injected into the stream for a period of 3.75 h. Samples were taken at various points downstream and flow was measured at the same time. Table 22 shows the simulation parameters.

Figure 22a to c demonstrate simulation results of Li concentration at 213 and 457 m stations, by three models. The figure and error indexes of Table 23 show that the results of the presented model have a better fit to observed data than the two other models. This figure also indicates that the general shape of the concentration-time curve for this example is a little different from the other examples; the reason for this can be attributed to the extreme changes in flow rate during experiment. Figure 22c presents the results of MIKE 11 model. As seen in figure, results have great discrepancies with observed data in peak concentrations and general shape of concentration-time curve. Figure 23 shows storage zone concentration at 213 and 457 m stations. As determined in figure, solute concentration-time curves in storage zone have lower peak and much

HESSD
12, 11959–12037, 2015

longer tails than main channel ones that indicates longer residence time of solute in these areas compared to main channel.

5 Sensitivity analysis

Two main input parameters to model, that describe the transient storage mechanism, includes cross-sectional area and exchange coefficient of storage area. The model results extremely depend on variations of these two parameters, so the sensitivity analysis of the proposed model to their changes is of great importance. For this purpose, a hypothetical example was designed and at first error indexes for base condition of sensitivity analysis determined for designed example. Then within the sensitivity analysis context, the desired parameter is changed in acceptable range and by keeping other parameters constant, model runs in this condition and error indexes evaluated.

Thus with obtaining error indexes due to desired parameter variations in sensitivity analysis in the form of a table, model sensitivity to desired parameter changes will be recognized. It should be noted that due to the high uncertainty in estimating the exchange coefficient with storage zone, a wide range of these parameter variations have been considered. According to error indexes provided in Table 24, it is clear that by increasing the cross-sectional area of storage zone, model accuracy is reduced. Because by increasing the area of this zone, the resident time in storage zone slightly increased and mass release will be delay awhile. The issue affects tail of concentration-time curve and makes it longer. The amount of delay is not remarkable, so it can be said that the model's sensitivity to changes in cross sectional area of storage zone is low (Fig. 24).

According to Table 25, it can be said that by increase and decrease of exchange coefficient relative to its value in the base case, model accuracy is reduced. The reason for this is that by increasing of exchange coefficient, solute concentration of storage zone increased significantly (Fig. 25) and consequently, the peak of main channel concentration-time curve fallen down and also the curve tail becomes longer and by re-

HESSD
12, 11959–12037, 2015

ducing this coefficient, contrary of that occurs, means that the curve be closer to curve that resulted from classical equation (excluding transient storage).

6 Conclusions

A literature review of solute transport modeling in natural streams and rivers show that despite of significant progress that has been made, there are still many problems that require further research, such that in the past most studies focused on solute transport under steady flow regime and regular sections that reflected as considering constant average velocity in the model. Whereas existence of unsteady flow and irregular cross sections are a common thing in natural streams and rivers. Another important point that neglected in the vast majority of current models is the impact of transient storage zones on solute transport process. Although already it is widely and increasingly accepted that for accurate simulation of solute transport in natural river and streams, the effect of transient storage zones must be taken into account and classical ADE equation in these cases has a serious weakness and inefficiency, still most common models using this equation in dealing with transport problem such as MIKE 11 software. Another case is the numerical method that used in the model structure. Since the numerical model gives an approximate solution of governing partial differential equations of phenomenon, accuracy, stability and flexibility of the solution is very important; hence providing models that can simulate solute transport under unsteady flow regime and irregular cross sections, and also have higher levels of accuracy and numerical stability, is necessary.

In this study a comprehensive model is presented, that merges numerical schemes with higher order accuracy for solution of advection-dispersion equation with transient storage zones in rivers with irregular cross sections at unsteady flow regime, to obviate the flaws in current models of contaminant transport simulation. For this purpose QUICK scheme due to high stability and law approximation errors have been used in spatial discretization of transport equation with transient storage and kinetic sorp-

HESSD
12, 11959–12037, 2015

tion. The presented method is verified by analytical solution for two types of boundary conditions and with considering transient storage and 2-D model. The results of verification implied that the presented model have reasonable accuracy in simulation of solute transport in natural river and streams with transient storage zones.

Then the model application was shown, compared to current common models in the form of two hypothetical examples and four sets of real data with different conditions (such as channel geometry, flow regime and the processes involved in transport). The results of first example showed that the numerical scheme used in the CTQS model, in cases where advection is the dominant transport process, have less numerical oscillations and higher stability compared to CTCS and BTCS numerical models. The results of second example indicate that quadratic upstream interpolation schemes such as QUICK scheme, expand the stability domain of numerical solution of solute transport equations (higher Peclet numbers) while maintaining an acceptable level of accuracy, can provide a larger grid size. While central spatial differencing method faced with step limitation and to achieve stable solution the calculation time step must be selected carefully, that in some practical applications will result in rise of computational cost.

The results of the third example for non-reactive tracer (chloride) showed that in addition to the standard mechanisms of advection and dispersion, transient storage mechanism also affects solute concentration levels at downstream. Results of the fourth example show that absorption of reactive tracer (strontium) in streambed sediments played role in reduction of concentrations levels at downstream. This is especially important in cases where pollution by fertilizers and pesticides occur, because the sorption of these substances into streambed sediments may greatly influence aquatic organisms and environment. Hence in order to achieve reliable prediction of pollutant transport the impact of storage zones and contaminant sorption into the streambed sediments must be considered. The fifth example presented to demonstrate the capability of model in accurate calculation of geometric properties of irregular cross-sections; the results indicate higher accuracy of model in simulation of solute transport in a river with irregular cross-sections and transient storage than two other models.

HESSD
12, 11959–12037, 2015

In the sixth example, the most complex possibility was considered. This example shows the model application and its results compared to the results of two other models in simulation solute transport under unsteady flow in a river with irregular cross-sections. This time, the results show again higher accuracy of the proposed model compared to other models. Then, the model sensitivity analysis also presented, to storage zone cross-sectional area and exchange coefficient variations. The results showed that the model is not sensitive to A_S variations, but has a relatively high sensitivity to changes in exchange rates of storage area, thus the choice of this parameter should be done to accomplish greater precision.

Overall, considering all the mentioned points and obtained results, it can be said that the presented model in this study is a comprehensive and practical model, that has the combined ability of solute transport simulation (reactive and non-reactive),with and without storage, under both steady and unsteady flow regimes, in rivers with irregular cross sections, without restrictions on the number of sections, that from this aspect, is unique compared to the other models that have been presented so far. Thus, it could be suggested as an appropriate alternative to the current popular models in solute transport studies in natural river and streams.

References

Avanzino, R. J., Zellweger, G., Kennedy, V., Zand, S., and Bencala, K.: Results of an solute transport experiment at Uvas Creek, September 1972, USGS Open-File Report 84-236 1984, p. 82, 40 fig, 9 tab, 5 ref, USGS, Menlo Park, California, 1984.

Bencala, K. E.: Simulation of solute transport in a mountain pool-and-riffle stream with a kinetic mass transfer model for sorption, Water Resour. Res., 19, 732–738, 1983.

Bencala, K. E.: Interactions of solutes and streambed sediment: 2. A dynamic analysis of coupled hydrologic and chemical processes that determine solute transport, Water Resour. Res., 20, 1804–1814, 1984.

Bencala, K. E. and Walters, R. A.: Simulation of solute transport in a mountain pool-and-riffle stream: a transient storage model, Water Resour. Res., 19, 718–724, 1983.

HESSD
12, 11959–12037, 2015

Bencala, K. E., Mcknight, D. M., and Zellweger, G. W.: Characterization of transport in an acidic and metal-rich mountain stream based on a lithium tracer injection and simulations of transient storage, Water Resour. Res., 26, 989–1000, 1990.
Chapra, S. C. and Runkel, R. L.: Modeling impact of storage zones on stream dissolved oxygen, J. Environ. Eng.-ASCE, 125, 415–419, 1999.
Chapra, S. C. and Wilcock, R. J.: Transient storage and gas transfer in lowland stream, J. Environ. Eng.-ASCE, 126, 708–712, 2000.
Czernuszenko, W. and Rowinski, P.: Properties of the dead-zone model of longitudinal dispersion in rivers, J. Hydraul. Res., 35, 491–504, 1997.
Czernuszenko, W., Rowinski, P.-M., and Sukhodolov, A.: Experimental and numerical validation of the dead-zone model for longitudinal dispersion in rivers, J. Hydraul. Res., 36, 269–280, 1998.
D'Angelo, D., Webster, J., Gregory, S., and Meyer, J.: Transient storage in Appalachian and Cascade mountain streams as related to hydraulic characteristics, J. N. Am. Benthol. Soc., 12, 223–235, 1993.
Day, T. J.: Longitudinal dispersion in natural channels, Water Resour. Res., 11, 909–918, 1975.
DeAngelis, D., Loreau, M., Neergaard, D., Mulholland, P., and Marzolf, E.: Modelling nutrient-periphyton dynamics in streams: the importance of transient storage zones, Ecol. Model., 80, 149–160, 1995.
Ensign, S. H. and Doyle, M. W.: In-channel transient storage and associated nutrient retention: evidence from experimental manipulations, Limnol. Oceanogr., 50, 1740–1751, 2005.
Fernald, A. G., Wigington, P., and Landers, D. H.: Transient storage and hyporheic flow along the Willamette River, Oregon: field measurements and model estimates, Water Resour. Res., 37, 1681–1694, 2001.
Godfrey, R. G. and Frederick, B. J.: Stream dispersion at selected sites, US Government Printing Office, Washington, D.C., 1970.
Gooseff, M. N., Hall, R. O., and Tank, J. L.: Relating transient storage to channel complexity in streams of varying land use in Jackson Hole, Wyoming, Water Resour. Res., 43, W01417, doi:10.1029/2005WR004626, 2007.
Harvey, J. W. and Wagner, B. J.: Quantifying hydrologic interactions between streams and their subsurface hyporheic zones, in: Streams and Ground Waters, edited by: Jones, J. A. and Mulholland, P. J., Academic Press, San Diego, USA, 3–44, 2000.

HESSD
12, 11959–12037, 2015

Jackman, A., Walters, R., and Kennedy, V.: Transport and concentration controls for chloride, strontium, potassium and lead in Uvas Creek, a small cobble-bed stream in Santa Clara County, California, USA: 2. Mathematical modeling, J. Hydrol., 75, 111–141, 1984.
Jin, L., Siegel, D. I., Lautz, L. K., and Otz, M. H.: Transient storage and downstream solute transport in nested stream reaches affected by beaver dams, Hydrol. Process., 23, 2438–2449, 2009.
Kazezyilmaz-Alhan, C. M.: Analytical solutions for contaminant transport in streams, J. Hydrol., 348, 524–534, 2008.
Keefe, S. H., Barber, L. B., Runkel, R. L., Ryan, J. N., Mcknight, D. M., and Wass, R. D.: Conservative and reactive solute transport in constructed wetlands, Water Resour. Res., 40, W01201 doi:10.1029/2003WR002130, 2004.
Laenen, A. and Bencala, K. E.: transient storage assessments of dye-tracer injections in rivers of the Willamette basin, Oregon, J. Am. Water Resour. As., 37, 367–377, 2001.
Leonard, B. P.: A stable and accurate convective modelling procedure based on quadratic upstream interpolation, Comput. Method. Appl. M., 19, 59–98, 1979.
Lin, Y.-C. and Medina Jr., M. A.: Incorporating transient storage in conjunctive stream–aquifer modeling, Adv. Water Resour., 26, 1001–1019, 2003.
Morrice, J. A., Valett, H., Dahm, C. N., and Campana, M. E.: Alluvial characteristics, groundwater–surface water exchange and hydrological retention in headwater streams, Hydrol. Process., 11, 253–267, 1997.
Neumann, L., Šimunek, J., and Cook, F.: Implementation of quadratic upstream interpolation schemes for solute transport into HYDRUS-1D, Environ. Modell. Softw., 26, 1298–1308, 2011.
Nordin, C. F. and Sabol, G. V.: Empirical data on longitudinal dispersion in rivers, Water-Resources Investigations Report 74-20, US Geological Survey, USA, 372 pp., 1974.
Nordin, C. F. and Troutman, B. M.: Longitudinal dispersion in rivers: the persistence of skewness in observed data, Water Resour. Res., 16, 123–128, 1980.
Putz, G. and Smith, D. W.: Two-dimensional modelling of effluent mixing in the Athabasca River downstream of Weldwood of Canada Ltd., University of Alberta, Hinton, Alberta, 2000.
Ramaswami, A., Milford, J. B., and Small, M. J.: Integrated Environmental Modeling: Pollutant Transport, Fate, and Risk in the Environment, J. Wiley, Hoboken, New Jersey, 2005.

HESSD
12, 11959–12037, 2015

Runkel, R. L.: One-dimensional Transport with Inflow and Storage (OTIS): a olute transport model for streams and rivers, Water-Resources Investigations Report, US Geological Survey, Denver, Colorado, 1998.
Runkel, R. L., Mcknight, D. M., and Andrews, E. D.: Analysis of transient storage subject to unsteady flow: diel flow variation in an Antarctic stream, J. N. Am. Benthol. Soc., 17, 143–154, 1998.
Scott, D. T., Gooseff, M. N., Bencala, K. E., and Runkel, R. L.: Automated calibration of a stream solute transport model: implications for interpretation of biogeochemical parameters, J. N. Am. Benthol. Soc., 22, 492–510, 2003.
Singh, S. K.: Treatment of stagnant zones in riverine advection-dispersion, J. Hydraul. Eng.-ASCE, 129, 470–473, 2003.
Szymkiewicz, R.: Numerical Modeling in Open Channel Hydraulics, Springer, Dordrecht, Heidelberg, London, New York, 2010.
Taylor, G.: The dispersion of matter in turbulent flow through a pipe, P. Roy. Soc. Lond. A, 223, 446–468, 1954.
Van Mazijk, A. and Veling, E.: Tracer experiments in the Rhine Basin: evaluation of the skewness of observed concentration distributions, J. Hydrol., 307, 60–78, 2005.
Versteeg, H. K. and Malalasekera, W.: An Introduction to Computational Fluid Dynamics: the Finite Volume Method, Pearson Education, Bell & Bain Ltd, Glasgow, UK, 2007.
Wagner, B. J. and Harvey, J. W.: Experimental design for estimating parameters of rate-limited mass transfer: analysis of stream tracer studies, Water Resour. Res., 33, 1731–1741, 1997.
Zhang, Y. and Aral, M. M.: Solute transport in open-channel networks in unsteady flow regime, Environ. Fluid Mech., 4, 225–247, 2004.

HESSD
12, 11959–12037, 2015

Table 1. Qualified comparison of three model characteristics.

Model	Model features				
	No limitations on the number of input parameters	Calculation of irregular cross-sections geometric properties	Unsteady flow sub-model	Transient storage	Kinetic sorption
Presented study	+	+	+	+	+
OTIS	–	–	–	+	+
MIKE 11	+	+	+	–	–

Note: the + sign means having a characteristic and symbol – means lack of it.

HESSD
12, 11959–12037, 2015

Table 2. Comparison of numerical methods used in structures of three models.

Model	Numerical methods			
	Discretization scheme	Accuracy order	Stability	Numerical dispersion
Present study	Centered Time – QUICK Space (CTQS)	Second order in time Third order in space	$Pe < 8/3$	–
OTIS	Centered Time – Centered Space (CTCS)	Second order in time second order in space	$Pe < 2$	–
MIKE 11	Backward Time – Centered Space (BTCS)	first order in time second order in space	$Pe < 2$	$U^2 \Delta t/2$

$Pe = u \cdot \Delta x / D$

HESSD
12, 11959–12037, 2015

Table 3. Characteristics of hypothetical examples for model verification.

Example	Verification method	Flow condition	Channel/river length (m)	Cross section type	Contaminant upstream boundary condition
First	Analytical solution	steady	200	Regular with constant area	Continuous in case 1 and case 2, Heaviside with 100 min, solute concentration at upstream boundary is 5 ($mg\,m^{-3}$) in both cases.
Second	2-D model	unsteady	1200	Irregular with varied area in space and time	Step load for 3 h and peak concentration is 20 ($mg\,m^{-3}$)

HESSD
12, 11959–12037, 2015

Table 4. Characteristics of hypothetical example for model verification by analytical solution.

Parameter	L (m)	Q ($m^3 s^{-1}$)	A_S (m^2)	A (m^2)	D ($m^2 s^{-1}$)	α (s^{-1})
	200	0.01	1	1	0.2	0.00002

HESSD
12, 11959–12037, 2015

Table 5. Error indexes for continuous boundary condition.

Index	Distance from upstream		
	50 m	75 m	100 m
R^2 (%)	99.97	99.96	99.96
RMSE ($mg\,m^{-3}$)	0.021	0.026	0.0326
MAE ($mg\,m^{-3}$)	0.0168	0.0227	0.029
MRE (%)	0.45	0.78	1.2

HESSD
12, 11959–12037, 2015

Table 6. Error indexes for continuous boundary condition, for simulations with and without transient storage.

Index	Distance from upstream 100 m	
	With storage	Without storage
R^2 (%)	99.96	99.99
RMSE ($mg\,m^{-3}$)	0.0326	0.0093
MAE ($mg\,m^{-3}$)	0.029	0.0065
MRE (%)	1.2	0.64

HESSD
12, 11959–12037, 2015

Table 7. Error indexes for Heaviside boundary condition.

Index	Distance from upstream		
	50 m	75 m	100 m
R^2 (%)	99.98	99.97	99.96
RMSE ($mg\,m^{-3}$)	0.034	0.045	0.058
MAE ($mg\,m^{-3}$)	0.031	0.0438	0.056
MRE (%)	3.5	4.2	5

HESSD
12, 11959–12037, 2015

Table 8. Error indexes for Heaviside boundary condition, for simulations with and without transient storage.

Index	Distance from upstream 100 m	
	With storage	Without storage
R^2 (%)	99.96	99.99
RMSE ($mg\,m^{-3}$)	0.058	0.0094
MAE ($mg\,m^{-3}$)	0.056	0.0075
MRE (%)	5	1.49

HESSD
12, 11959–12037, 2015

Table 9. Characteristics of hypothetical example for model verification with 2-D model.

Parameter	n ($s m^{-1/3}$)	D ($m^2 s^{-1}$)	A_S (m^2)	α (s^{-1})	DaI
	0.025	10	22	1.8×10^{-4}	0.4

HESSD
12, 11959–12037, 2015

Table 10. Error indexes for CTQS, CTCS and BTCS methods for verification with 2-D model.

Index	Distance from upstream, 500 m		
	CTCS	BTCS	CTQS
R^2 (%)	99.36	99.37	99.43
RMSE ($mg\,m^{-3}$)	0.36	0.37	0.35
MAE ($mg\,m^{-3}$)	0.16	0.18	0.15
MRE (%)	8.6	12.15	6.09

HESSD
12, 11959–12037, 2015

Table 11. The examples used for demonstration of model application.

Example	Section type	Flow regime	Solute transport processes					
			Physical				Chemical	
					Transient storage			
			Advection	Dispersion	Surface decay	Hyporheic exchange	First-order dacay	Kinetic sorption
1	regular	Steady uniform	+	–	–	–	–	–
2	regular	Steady uniform	+	+	–	–	+	–
3	irregular	Steady non-uniform	+	+	+	–	–	–
4	irregular	Steady non-uniform	+	+	+	–	–	+
5	irregular	Steady uniform	+	+	+	–	–	–
6	irregular	unsteady non-uniform	+	+	–	+	–	–

Note: + sign means that the process affects transport and – sign means no effect.

HESSD
12, 11959–12037, 2015

Table 12. Characteristics of example 2.

Parameter	L (m)	Q ($\mathrm{L\,s^{-1}}$)	A ($\mathrm{m^2}$)	D ($\mathrm{m^2\,s^{-1}}$)	λ ($\mathrm{s^{-1}}$)
	2200	0.12	1	5	0.00002

HESSD
12, 11959–12037, 2015

Table 13. Characteristics of three cases of models implementation.

Case	Space step (m)	Flow velocity ($m s^{-1}$)	Peclet number
1	10	0.12	0.24
2	100	0.12	2.4
3	100	0.5	10

HESSD
12, 11959–12037, 2015

Table 14. Error indexes for concentration time profiles in 500 m from upstream.

	Index	Distance from upstream, 500 m		
		CTQS	OTIS	MIKE11
Case 1	R^2 (%)	99.93	99.93	99.98
	RMSE	0.46	0.46	0.85
	MAE	0.236	0.238	0.48
	MRE (%)	0.9	1	1.7
Case 2	R^2 (%)	98.26	97.82	97.75
	RMSE	2.66	2.98	3.24
	MAE	1.42	1.55	1.73
	MRE (%)	3.77	4.11	4.93
Case 3	R^2 (%)	98.8	98.2	98.24
	RMSE	3.6	4.41	4.46
	MAE	0.8	1.12	1.17
	MRE (%)	1.25	1.95	2.15

HESSD
12, 11959–12037, 2015

Table 15. Error indexes for concentration space profile.

	Index	Distance from upstream, 500 m		
		CTQS	OTIS	MIKE11
Case 1	R^2 (%)	99.9	99.9	99.9
	RMSE	0.146	0.154	0.36
	MAE	0.105	0.108	0.28
	MRE (%)	1.91	1.97	3.2
Case 2	R^2 (%)	98.6	98	96
	RMSE	0.53	0.65	0.86
	MAE	0.4	0.47	0.64
	MRE (%)	5.4	6.56	11.2
Case 3	R^2 (%)	95.7	92	88.4
	RMSE	5.46	7.24	7.88
	MAE	3.02	4.47	5.05
	MRE (%)	6.27	12.44	13.5

HESSD
12, 11959–12037, 2015

Table 16. Simulation parameters for Uvas Creek experiment.

Reach (m)	Flow discharge ($m^3 s^{-1}$)	Dispersion coefficient ($m^2 s^{-1}$)	Cross-sectional areas		Exchange coefficient
			Main channel	Storage zone	
0–38	0.0125	0.12	0.3	0	0
38–105	0.0125	0.15	0.42	0	0
105–281	0.0133	0.24	0.36	0.36	3×10^{-5}
281–433	0.0136	0.31	0.41	0.41	1×10^{-5}
433–619	0.0140	0.4	0.52	1.56	4.5×10^{-5}

HESSD
12, 11959–12037, 2015

Table 17. Example 2 error indexes.

Index	38 m			281 m			433 m		
	CTQS	OTIS	MIKE11	CTQS	OTIS	MIKE11	CTQS	OTIS	MIKE11
R^2 (%)	94.3	94.2	94.1	99.4	99.31	99.1	98.84	98.8	97.82
RMSE ($mg\,m^{-3}$)	0.727	0.728	0.73	0.18	0.183	0.34	0.203	0.205	0.44
MAE ($mg\,m^{-3}$)	0.202	0.203	0.212	0.108	0.109	0.205	0.121	0.125	0.28
MRE (%)	3.5	3.55	3.68	2.075	2.08	3.6	2.27	2.4	5.3

HESSD
12, 11959–12037, 2015

Table 18. Simulation parameters of example 3.

Distribution coefficient, K_d ($m^2\,s^{-1}$)	sorption rate coefficient (s^{-1})		Background concentration ($mg\,L^{-1}$)			Input concentration ($mg\,L^{-1}$)
	Main channel	Storage zone	Main channel	Storage zone	Bed sediments	
70	56×10^{-6}	1	0.13	0.13	9.1×10^{-3}	1.73

HESSD
12, 11959–12037, 2015

Table 19. Error indexes of 38, 281 and 433 m stations in example 3.

Index	38 m			281 m			433 m		
	CTQS	OTIS	MIKE11	CTQS	OTIS	MIKE11	CTQS	OTIS	MIKE11
R^2 (%)	99.3	93.17	93	99	96	90.8	93.6	90	80.2
RMSE ($mg\,m^{-3}$)	0.05	0.12	0.17	0.055	0.07	0.2	0.06	0.067	0.26
MAE ($mg\,m^{-3}$)	0.021	0.044	0.086	0.048	0.055	0.115	0.05	0.06	0.15
MRE (%)	6.4	11.8	24.6	13.6	18	27.4	17.4	20.7	40

HESSD
12, 11959–12037, 2015

Table 20. Error indexes of 105 and 281 m stations in example 3.

Index	105 m		281 m	
	CTQS	OTIS	CTQS	OTIS
R^2 (%)	99.4	99.3	99.16	98.6
RMSE ($mg\,m^{-3}$)	1.05	1.64	2.67	2.86
MAE ($mg\,m^{-3}$)	0.75	1.5	2.4	2.41
MRE (%)	3.04	5.66	10.5	10.8

HESSD
12, 11959–12037, 2015

Table 21. Error indexes of Athabasca River experiment.

Index	Distance from upstream, 1850 m		
	CTQS	OTIS	MIKE11
R^2 (%)	99.75	99.8	62.5
RMSE ($mg\,m^{-3}$)	0.03	0.047	0.5
MAE ($mg\,m^{-3}$)	0.02	0.025	0.26
MRE (%)	1.7	4.77	28.6

HESSD
12, 11959–12037, 2015

Table 22. Simulation parameters of Huey Creek.

Reach (m)	Dispersion coefficient ($m^2 s^{-1}$)	Storage zone cross-sectional area	Exchange coefficient
0–213	0.5	0.2	1.07×10^{-3}
213–457	0.5	0.25	5.43×10^{-4}
457–726	0.5	0.14	1.62×10^{-2}

HESSD
12, 11959–12037, 2015

Table 23. Huey Creek experiment error indexes.

Index	213 m			457 m		
	CTQS	OTIS	MIKE11	CTQS	OTIS	MIKE11
R^2 (%)	68.6	67	84	78	63.5	94
RMSE ($mg\,m^{-3}$)	0.673	0.674	0.74	0.48	0.63	0.62
MAE ($mg\,m^{-3}$)	0.28	0.3	0.54	0.23	0.28	0.52
MRE (%)	7.14	7.32	20.4	6.46	7.6	15

HESSD
12, 11959–12037, 2015

Table 24. Model sensitivity analysis to variations of cross sectional area of storage zone.

Index	Storage zone cross-sectional area (m)						
	$A_S - 30\,\%$	$A_S - 20\,\%$	$A_S - 10\,\%$	A_S	$A_S + 10\,\%$	$A_S + 20\,\%$	$A_S + 30\,\%$
R^2 (%)	99.53	99.49	99.46	99.43	99.39	99.35	99.3
RMSE ($mg\,m^{-3}$)	0.34	0.354	0.365	0.37	0.39	0.4	0.416
MAE ($mg\,m^{-3}$)	0.17	0.173	0.176	0.179	0.183	0.188	0.193
MRE (%)	6.16	6.2	6.23	6.36	6.363	6.365	6.37

HESSD
12, 11959–12037, 2015

Table 25. Model sensitivity analysis to variations of exchange coefficient of storage zone.

Index	Storage zone exchange coefficient (s^{-1})						
	$1/4\alpha$	$1/3\alpha$	$1/2\alpha$	α	2α	3α	4α
R^2 (%)	99.3	99.32	99.36	99.43	99.47	99.5	99.52
RMSE ($mg\,m^{-3}$)	0.45	0.43	0.41	0.37	0.415	0.51	0.62
MAE ($mg\,m^{-3}$)	0.202	0.196	0.187	0.179	0.23	0.29	0.345
MRE (%)	7.15	7	6.74	6.36	754	8.59	9.73

HESSD
12, 11959–12037, 2015

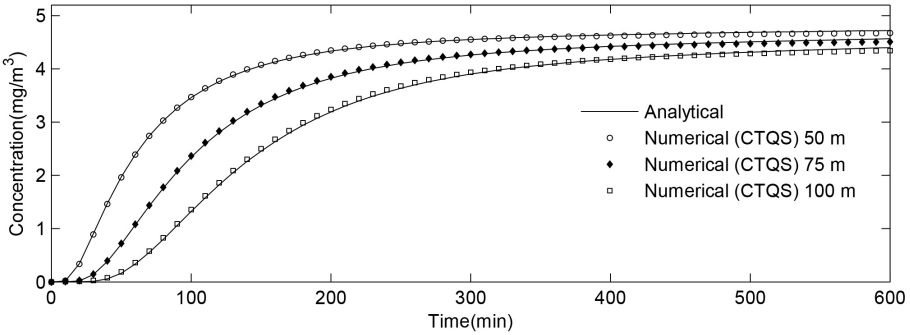

Figure 1. Results of model verification by analytical solution for continuous boundary condition, at 50, 75 and 100 m from upstream.

HESSD
12, 11959–12037, 2015

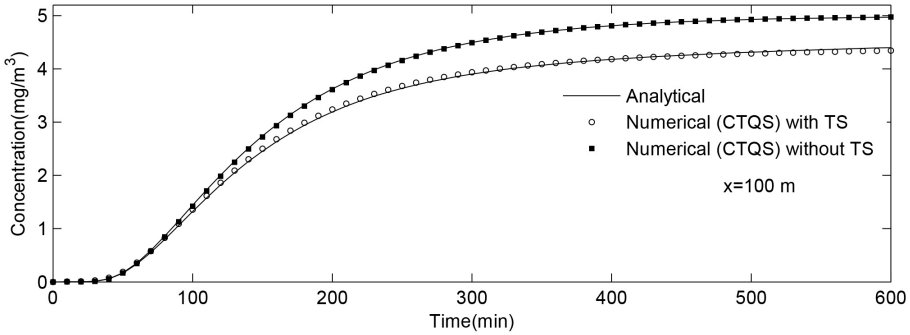

Figure 2. Model verification results with analytical solution for continuous boundary condition, for simulations with and without transient storage, at 100 m from upstream.

HESSD
12, 11959–12037, 2015

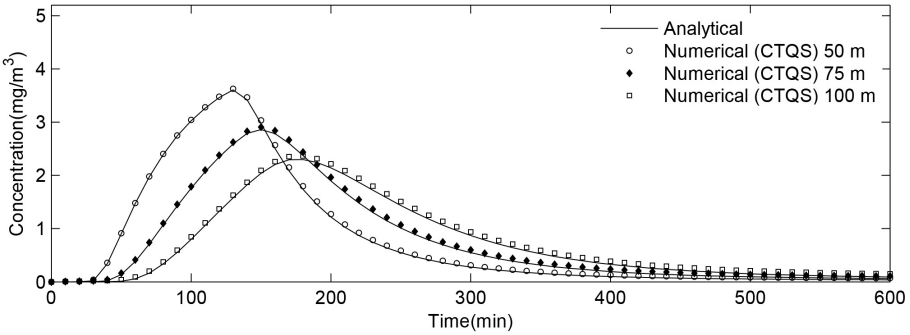

Figure 3. Results of model verification with analytical solution for Heaviside boundary condition, at 50, 75 and 100 m from upstream.

HESSD
12, 11959–12037, 2015

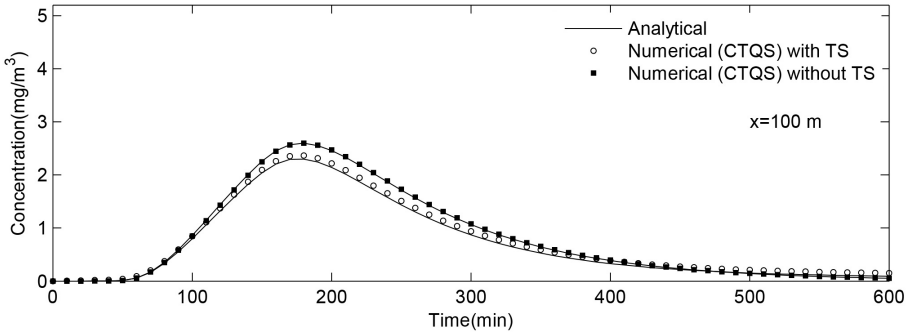

Figure 4. Model verification results with analytical solution for Heaviside boundary condition, for simulations with and without transient storage, at 100 m from upstream.

HESSD
12, 11959–12037, 2015

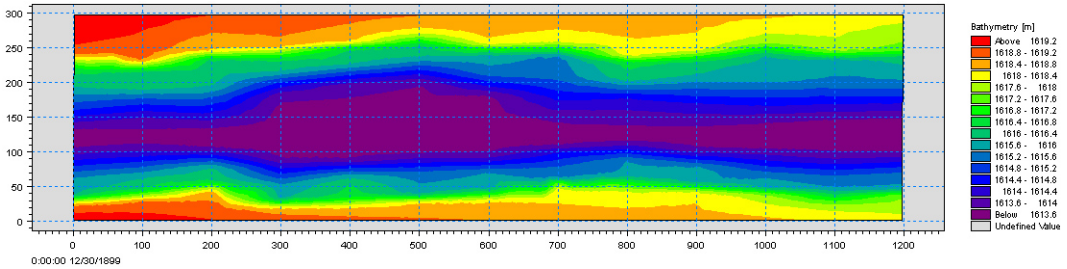

Figure 5. Bathymetry properties of hypothetical river.

HESSD
12, 11959–12037, 2015

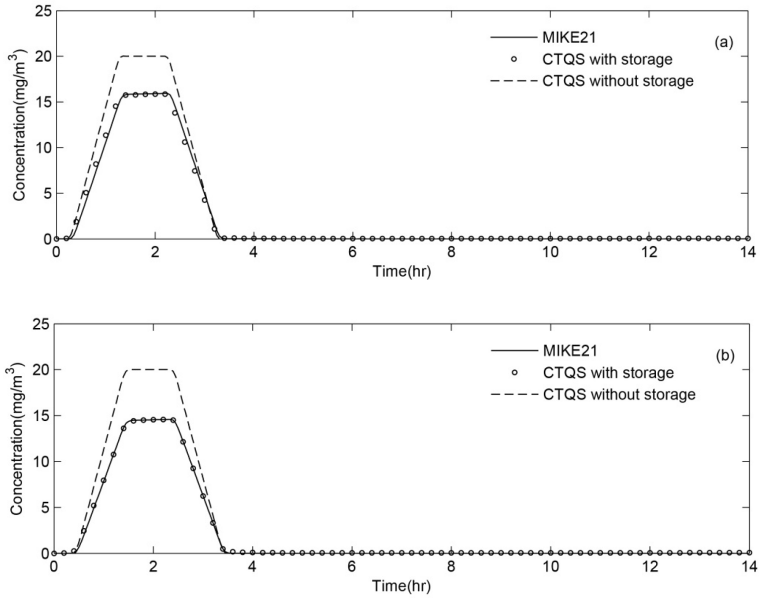

Figure 6. Simulation results of CTQS method for simulation with and without storage in compare with 2-D model results at **(a)** 500 m and **(b)** 800 m from channel upstream.

HESSD
12, 11959–12037, 2015

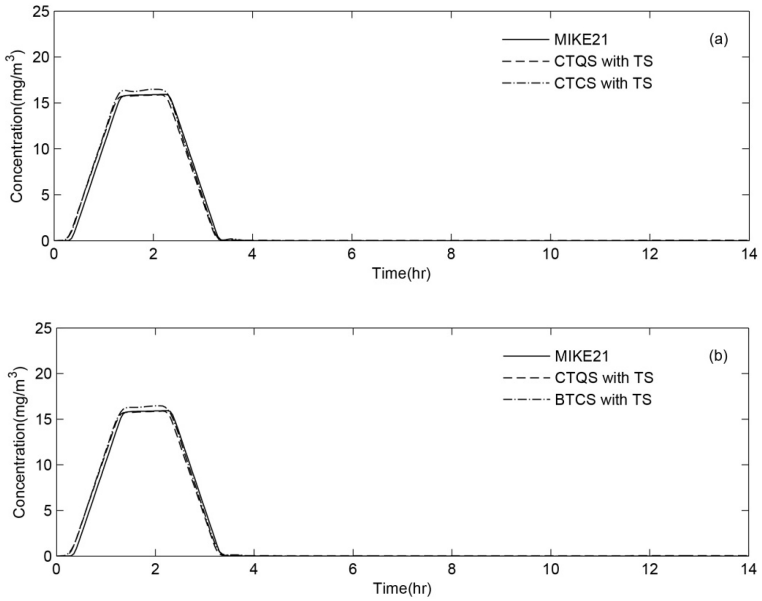

Figure 7. Comparison of results of **(a)** CTQS and CTCS, **(b)** CTQS and BTCS models with 2-D model ones at 500 m from upstream.

HESSD
12, 11959–12037, 2015

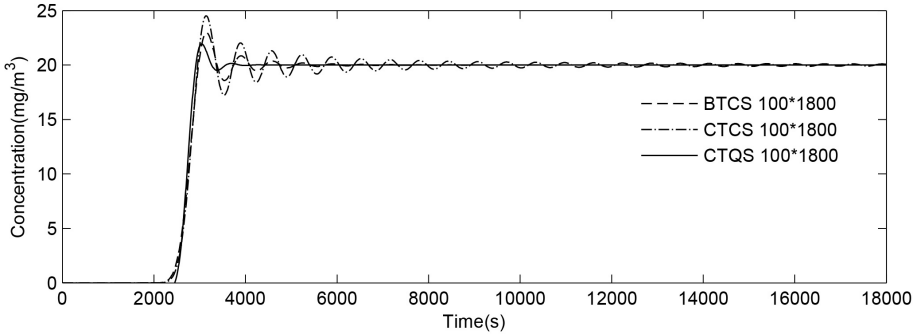

Figure 8. Comparison of CTQS, CTCS and BTCS scheme results for pure advection simulation at 100 × 1800 computation grid.

HESSD
12, 11959–12037, 2015

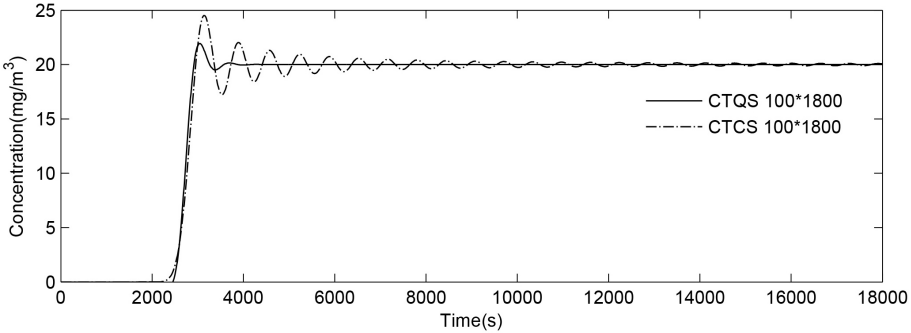

Figure 9. Comparison of CTQS and CTCS scheme results for pure advection simulation at 100 × 1800 computation grid.

HESSD
12, 11959–12037, 2015

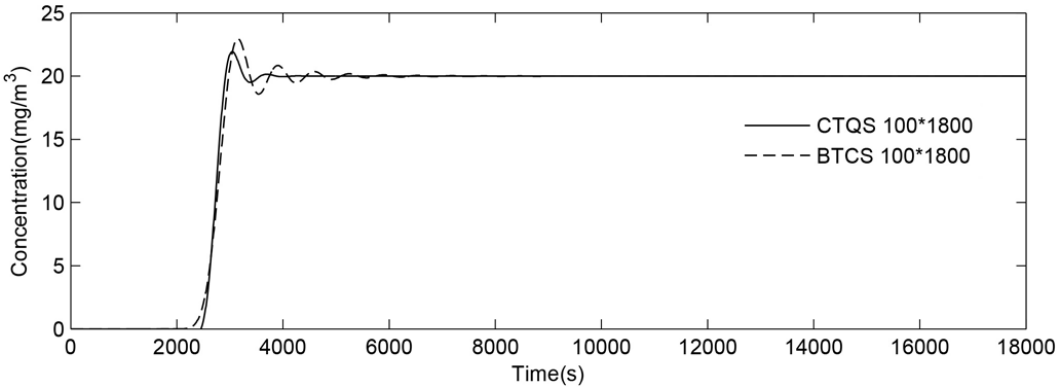

Figure 10. Comparison of CTQS and BTCS scheme results for pure advection simulation at 100 × 1800 computation grid.

HESSD
12, 11959–12037, 2015

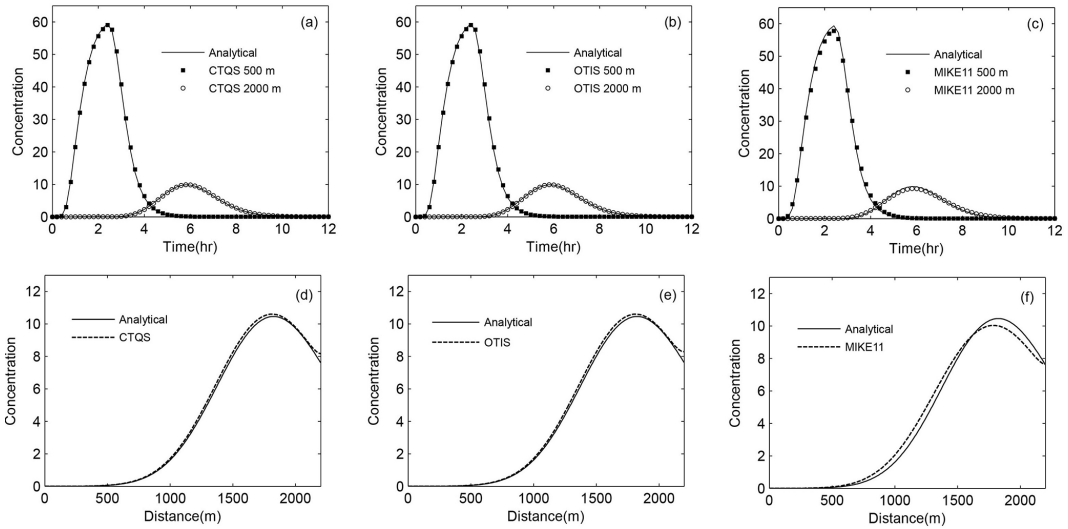

Figure 11. Comparison of various numerical schemes (CTQS, OTIS and MIKE11) with analytical solution for the first case.

HESSD
12, 11959–12037, 2015

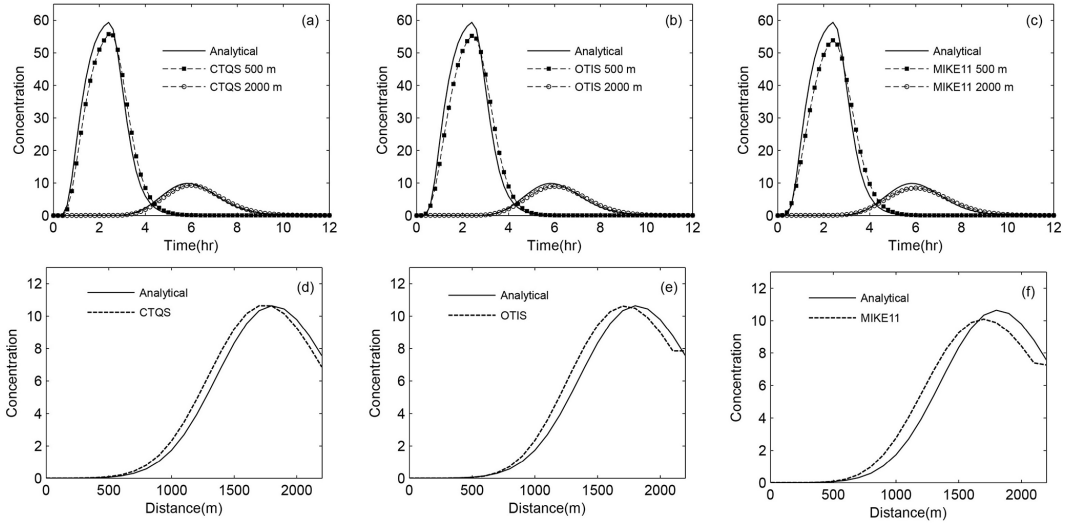

Figure 12. Comparison of various numerical schemes (CTQS, OTIS and MIKE11) with analytical solution for the second case.

HESSD
12, 11959–12037, 2015

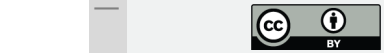

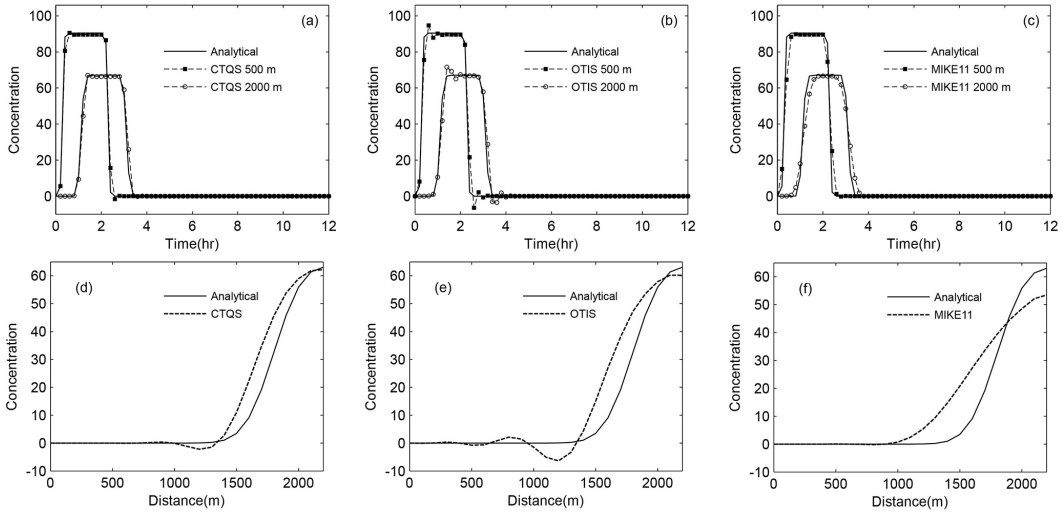

Figure 13. Comparison of various numerical schemes (CTQS, OTIS and MIKE11) with analytical solution for the third case.

HESSD
12, 11959–12037, 2015

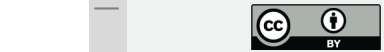

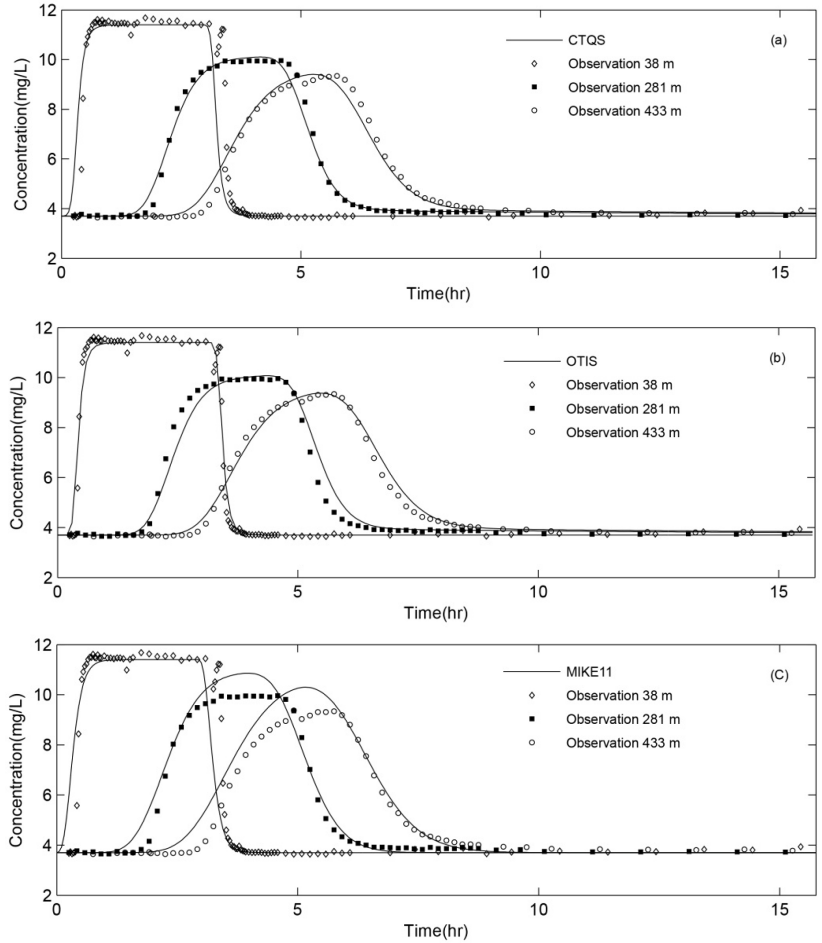

Figure 14. Observed and simulated chloride concentrations in main channel at 38, 281 and 433 m Uvas Creek by **(a)** CTQS, **(b)** OTIS and **(c)** MIKE11 models.

HESSD
12, 11959–12037, 2015

One-dimensional numerical model for solute transport in rivers

M. Barati Moghaddam et al.

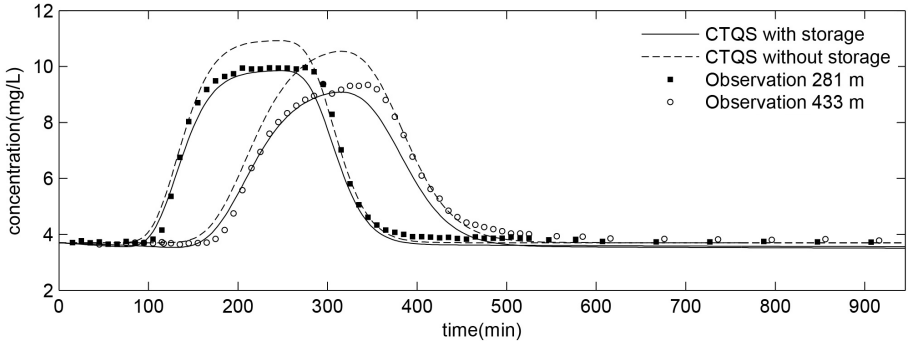

Figure 15. CTQS model results for simulation with and without transient storage at 281 and 433 m stations.

HESSD
12, 11959–12037, 2015

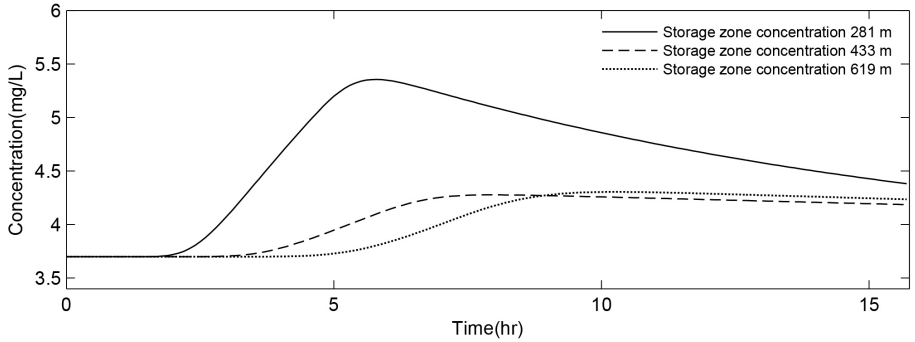

Figure 16. Observes and simulated chloride concentrations at 281, 433 and 619 m stations.

HESSD
12, 11959–12037, 2015

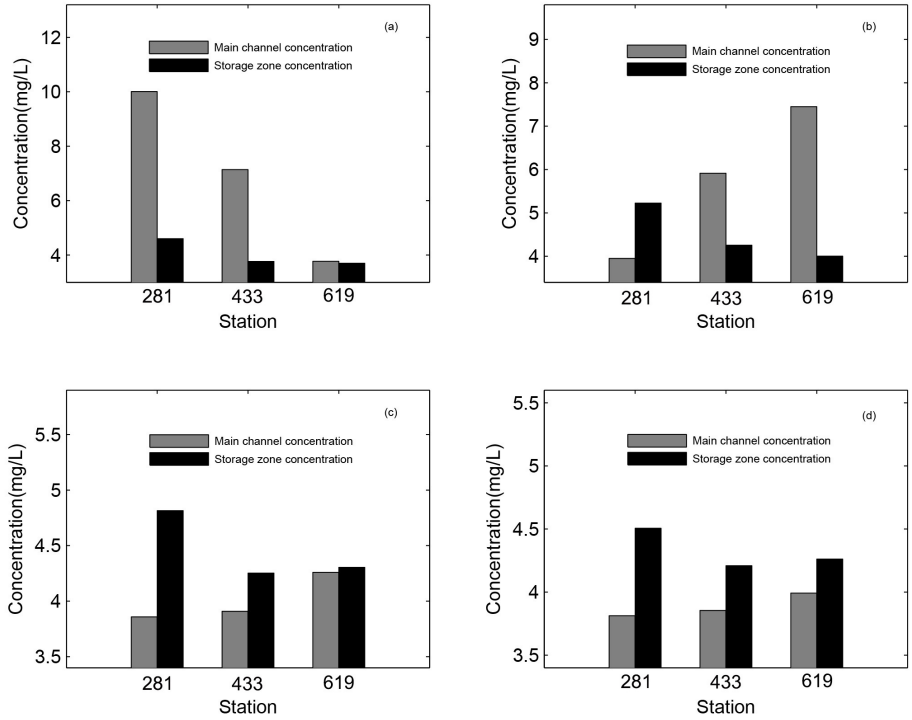

Figure 17. Comparison of main channel concentration (left column) and storage zone (right column) at 281, 433 and 619 m Uvas Creek in various times **(a)** 4.5 **(b)** 7, **(c)** 5 and **(d)** 15 h after simulation start.

HESSD
12, 11959–12037, 2015

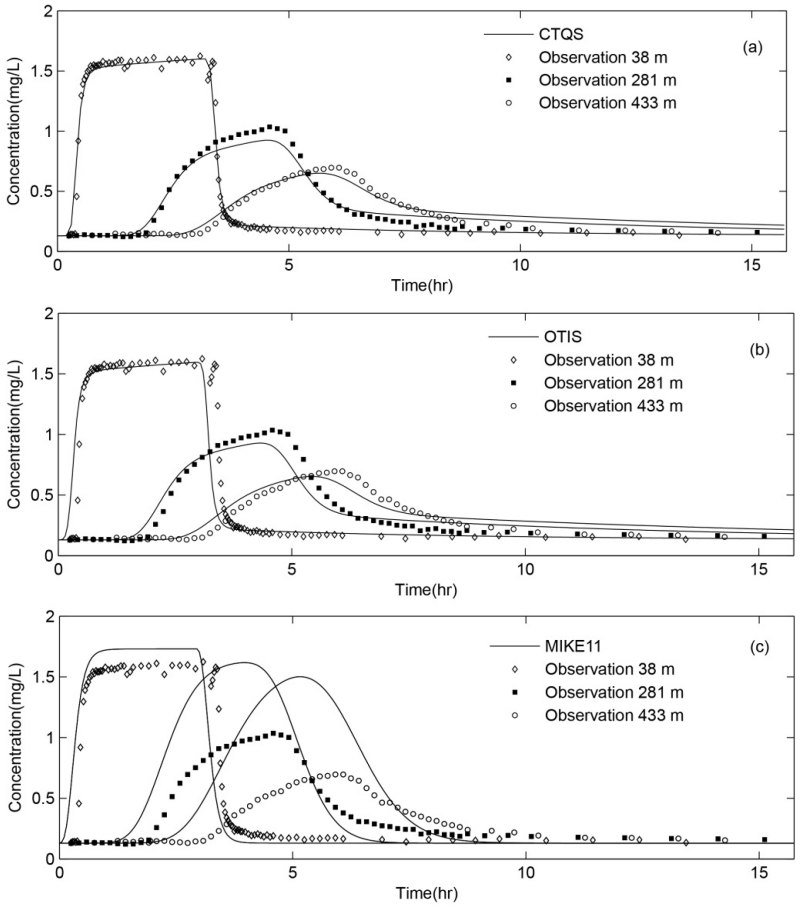

Figure 18. Observed and simulated Strontium concentrations in main channel affected by various physical and chemical processes at 38, 281 and 433 m Uvas Creek by **(a)** CTQS, **(b)** OTIS and **(c)** MIKE11 model.

HESSD
12, 11959–12037, 2015

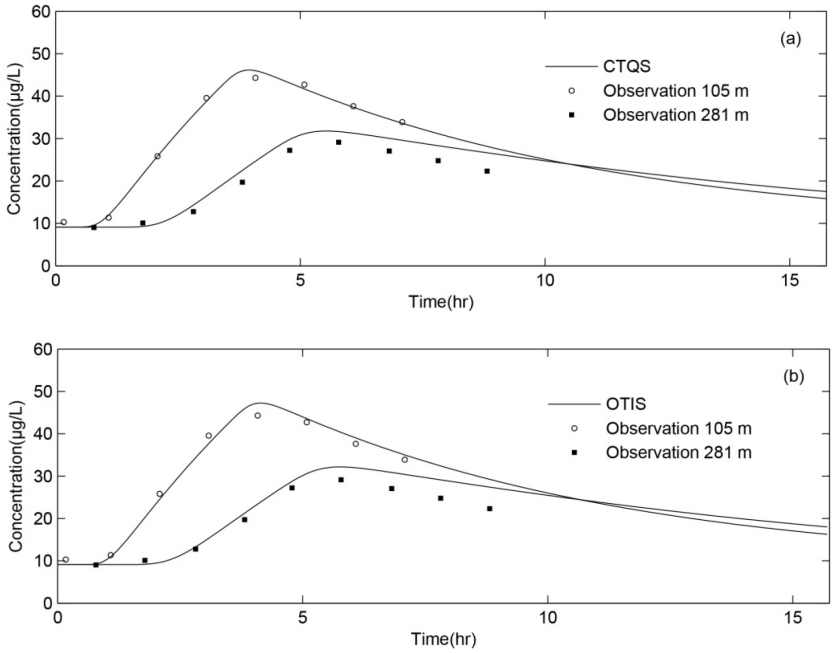

Figure 19. Sorbate and observed Strontium concentrations at 105 and 281 m stations of Uvas Creek by **(a)** CTQS and **(b)** OTIS model.

HESSD
12, 11959–12037, 2015

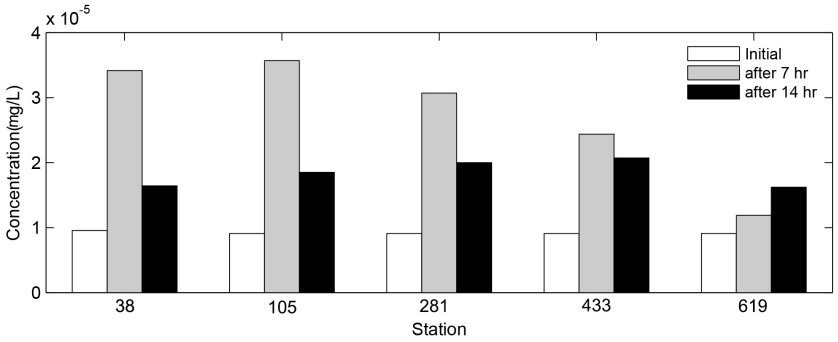

Figure 20. Sorbate concentrations of Strontium at various times at five observation stations of Uvas Creek.

HESSD
12, 11959–12037, 2015

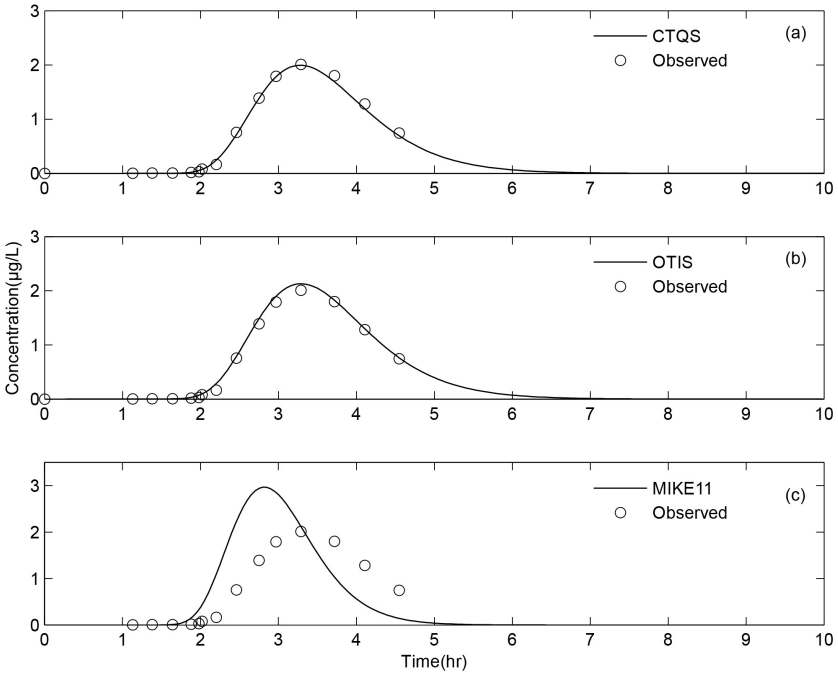

Figure 21. Simulation results for Athabasca River experiment at 11.85 km downstream from injection point by **(a)** CTQS, **(b)** OTIS and **(c)** MIKE11 model.

HESSD
12, 11959–12037, 2015

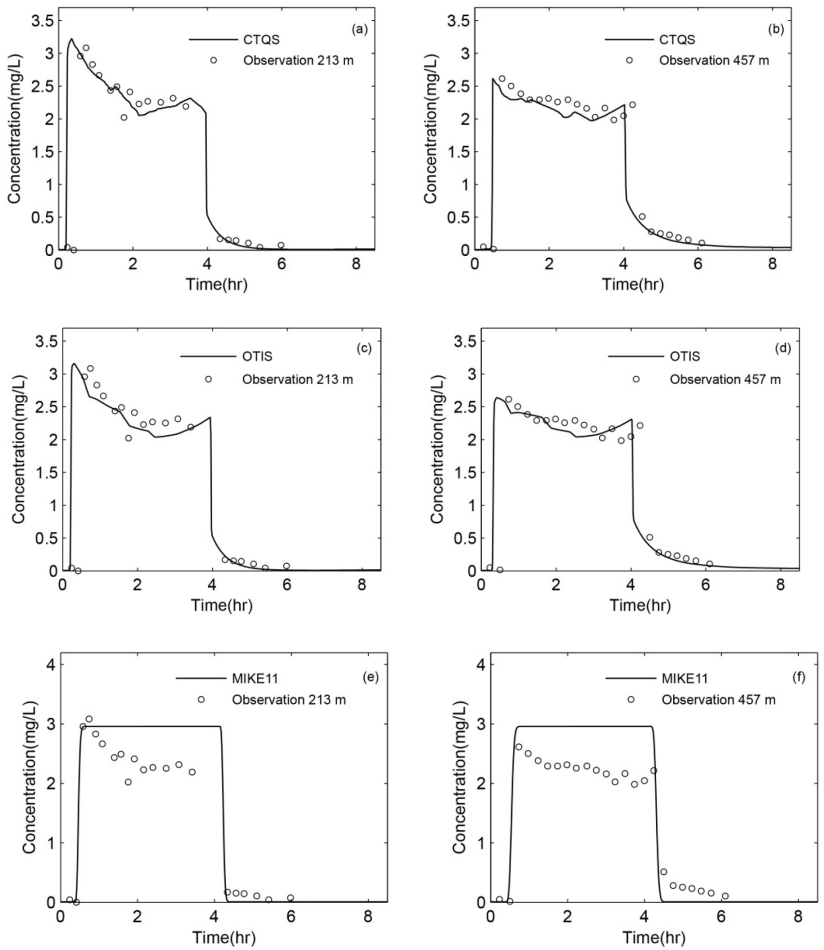

Figure 22. Observed and simulated main channel Li concentrations at 213 and 457 m stations of Huey Creek by **(a, b)** CTQS, **(c, d)** OTIS and **(f, e)** MIKE11 model.

HESSD
12, 11959–12037, 2015

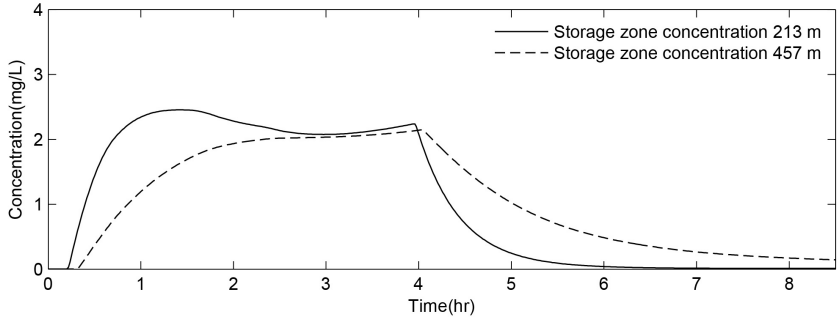

Figure 23. Storage zone concentration at 213 and 457 m station of Huey Creek.

HESSD
12, 11959–12037, 2015

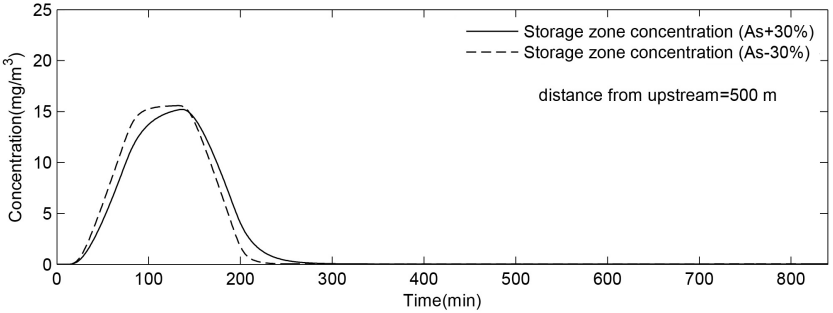

Figure 24. Comparison of transient storage zone concentrations at upper and lower limits of transient storage cross sectional area variations.

HESSD
12, 11959–12037, 2015

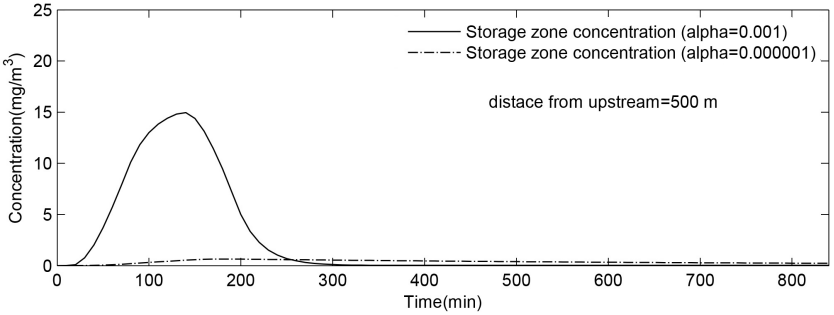

Figure 25. Comparison of transient storage zone concentrations at upper and lower limit of transient storage exchange coefficient.

HESSD
12, 11959–12037, 2015